

GRAMICIDIN A PEPTIDE CONFORMATIONS STUDIED BY ION MOBILITY -
MASS SPECTROMETRY

A Dissertation

by

JOHN W. PATRICK

Submitted to the Office of Graduate and Professional Studies of
Texas A&M University
in partial fulfillment of the requirements for the degree of

DOCTOR OF PHILOSOPHY

Chair of Committee,	David H. Russell
Committee Members,	Christian Hilty
	Karen Wooley
	Jean-Phillipe Pellois
Head of Department,	Simon North

May 2017

Major Subject: Chemistry

Copyright 2017 John W. Patrick

ABSTRACT

One of the most rapidly advancing subjects studied by analytical chemistry, biology, and biophysics is the analysis of membrane associated peptides and proteins from a native lipid environment. Mass spectrometry (MS) has been employed for many years as a tool to characterize the molecular weight, sequence, or modifications to these peptides and proteins, however MS alone does not provide information on the conformation adopted by a peptide or protein in the membrane. Here, novel sample preparation methods to probe the solution phase structure of dimerized Gramicidin A (GA) inserted into lipid vesicle bilayers are described. These methods, termed vesicle capture-freeze drying (VCFD) and mixing tee-ESI (MT-ESI), when coupled with electrospray ionization ion mobility mass spectrometry (ESI-IM-MS), successfully demonstrate the first evidence for the preservation of membrane-bound structure in the analysis of solution-phase conformers retained into the gas phase. The extremely hydrophobic character of GA ensures that only membrane-bound conformations are captured and subsequently monitored when samples are prepared using VCFD, removing a barrier that has prevented previous attempts at direct analysis using mass spectrometry. Solution-phase physico-chemical interactions of GA influenced by lipid acyl chain length and extent of acyl chain unsaturation can now be probed by monitoring the conformer preferences using IM-MS. Conformer preferences adopted in the lipid bilayer are maintained as GA dimers travel from the solution phase to fully desolvated gas-phase ions, demonstrating that distributions observed using ESI-IM-MS unambiguously reflect the ensemble of

conformers observed in the solution phase. The required time for GA sample preparation was decreased by approximately 50% using MT-ESI when compared to VCFD sample preparation; however, comparable conformer preferences were obtained using both techniques. GA analogues that contain leucine to lysine substitutions were analyzed; these analogues yielded more hydrophilic GA dimers owing to the hydrophilicity of lysine head groups. The conformer preferences of lipid bilayer associated hydrophilic GA analogues can be obtained owing to disassociation of lipids during the fast mixing time MT-ESI process. Both VCFD and MT-ESI coupled to IM-MS yield novel biophysical insight into the influence of lipid bilayer membranes on conformer preferences and conformer heterogeneity of an important channel-forming membrane peptide.

DEDICATION

This work is dedicated to my loving grandparents Jack and Jane Patrick as well as Pauline Waibel and to my parents, John and Paula, who worked hard to ensure I had the tools needed to succeed in my career.

ACKNOWLEDGEMENTS

I am incredibly appreciative of all those in the Russell Research Group who have helped foster my scientific skill set and taught me more than I could have hoped when I entered graduate school. Firstly, my thanks go to Dr. David H. Russell whose guidance and assistance has been a vital component of both my success in graduate school and my own personal growth. I would like to thank Dr. William K. Russell for his mentorship in the Laboratory for Biological Mass Spectrometry. I would like to thank Dr. Roberto C. Gamez for his assistance in lipid related research and for helping to strengthen the foundation of this project. Dr. Gregory Matthijetz for his constant assistance in tinkering with the items I have broken. Special thanks go to Dr. Pei Jing (Peggy) Pai, Dr. Shu-Hua Chen, and Dr. Fred Zinnel for their assistance with learning ion mobility applications. Thank you to my committee members Dr. Karen Wooley, Dr. Christian Hilty, and Dr. Jean-Phillipe Pellois for their expertise in guiding my thesis work. I would like to thank Dr. Paul Cremer for lending his laboratory space and those in the Cremer group at Texas A&M for the assistance in the early stages of my research. My sincere thanks to Dr. Jianmin Gao for his gracious donation of Gramicidin samples and aid in revising our collaborative work.

To all my friends and coworkers who have offered assistance, constructive criticism, or simply shared a warm cup of coffee with me over the years – I owe you my deepest thanks. The friendships I have made over the years at Texas A&M have profoundly shaped who I am today.

This work was supported by the National Institute of Health, Department of Energy, and National Science Foundation.

NOMENCLATURE

IMS	Ion Mobility Spectrometry
MS	Mass Spectrometry
IM-MS	Ion Mobility-Mass Spectrometry
CCS	Collision Cross Section
ESI	Electrospray Ionization
GA	Gramicidin A
ATD	Arrival Time Distribution
m/z	Mass-to-charge ratio
PDH	Parallel double helix
ADH	Antiparallel double helix
SSH	Single stranded head to head dimer
DGA	Deformylated Gramicidin A
SUV	Small unilamellar vesicle
TEM	Transmission Electron Microscopy
PL	Phospholipid
LBL	Lipid bilayer
VCFD	Vesicle capture – freeze drying
DLPC	(12:0, 12:0) 1,2-dilauroyl- <i>sn</i> -glycero-3-phosphocholine
DMPC	(14:0, 14:0) 1,2-dimyristoyl- <i>sn</i> -glycero-3-phosphocholine
DPPC	(16:0, 16:0) 1,2-dipalmitoyl- <i>sn</i> -glycero-3-phosphocholine
DOPC	(18:1, 18:1) 1,2-dioleoyl- <i>sn</i> -glycero-3-phosphocholine

POPC	(16:0, 18:1) 1-palmitoyl-2-oleoyl- <i>sn</i> -glycero-3-phosphocholine
DEPC	(22:1, 22:1) 1,2-dierucoyl- <i>sn</i> -glycero-3-phosphocholine
WT	Wild type

TABLE OF CONTENTS

	Page
ABSTRACT	ii
DEDICATION	iv
ACKNOWLEDGEMENTS	v
NOMENCLATURE.....	vii
TABLE OF CONTENTS	ix
LIST OF FIGURES.....	xi
CHAPTER I INTRODUCTION	1
The Utility of Mass Spectrometry in GA Characterization.....	2
Native Structure in Mass Spectrometry	2
Membrane Description.....	4
CHAPTER II METHODS.....	10
Comparable Techniques to ESI.....	16
Lipid Vesicle Preparation.....	17
Vesicle Imaging.....	18
Vesicle Capture – Freeze Drying	18
CHAPTER III ELUCIDATION OF CONFORMER PREFERENCES FOR A HYDROPHOBIC ANTIMICROBIAL PEPTIDE BY VESICLE CAPTURE- FREEZE DRYING: A NOVEL PREPARATORY METHOD COUPLED TO ION MOBILITY – MASS SPECTROMETRY	20
Introduction	20
Materials and Methods	23

Results and Discussion.....	26
Conclusion.....	37
CHAPTER IV THE INFLUENCE OF LIPID BILAYER PHYSICOCHEMICAL PROPERTIES ON THE CONFORMER PREFERENCES OF THE MODEL ION CHANNEL GRAMICIDIN A	38
Introduction	38
Materials and Methods	43
Results	47
Discussion.....	52
Conclusion.....	61
CHAPTER V RAPID CAPILLARY MIXING EXPERIMENTS FOR THE ANALYSIS OF HYDROPHOBIC MEMBRANE COMPLEXES DIRECTLY FROM AQUEOUS LIPID BILAYER SOLUTIONS.....	63
Introduction	63
Methods	65
Results and Discussion.....	66
Conclusions	78
CHAPTER VI SUMMARY AND FUTURE OUTLOOK	79
Summary	79
Future Directions.....	82
REFERENCES	85
APPENDIX	104

LIST OF FIGURES

	Page
Figure 1. Illustrations of three GA conformer families. Tryptophan sidechains at positions 9,11,13 and 15 are denoted in black.	5
Figure 2. Main components and layout of a typical TOF system with reflecting mass analyzer. The ion beam enters from a source at the left and is accelerated to enter the orthogonal accelerator (oa). The beam “fills” the first stage of the oa until a bipolar pushout pulse pair is applied. A packet of ions of length l_p is thus sampled and accelerated through grids to enter the drift region at a potential of V_{tof} . Reflecting TOF optics are used to bring the ions to a space-time focus on the detector. Reprinted with permission from Elsevier, Copyright 1993. ²⁷	9
Figure 3. Illustration of major processes in an ESI ion source run in the positive ion mode. An electric field penetrates into the liquid leading to an enrichment of positive ions present. Evaporation of the droplets brings the charges closer together. The increasing Coulombic repulsion destabilizes the droplets which emit jets of charged progeny droplets eventually forming free gas-phase ions. Reprinted with permission from Wiley Periodicals, Copyright 2009. ³³	11
Figure 4. Drift tube IM: In drift tube ion mobility, packets of ions traverse the cell along a potential gradient against a constant gas flow. Larger ions experience more collisions with the gas and therefore are retarded relative to smaller ions with a higher mobility. Reprinted with permission from Royal Society of Chemistry, Copyright 2001. ³⁶	13
Figure 5. A plot of IM-MS conformation space obtained for a mixture of model species representing each molecular class (ranging from seven to 17 model species for each class, spanning a range of masses up to 1,500 Da). Dashed lines are for visualization purposes of where each molecular class occurs in conformation space. Signals in the vicinity of the asterisk arise from limited	

post-IM fragmentation of the parent ion species. Reprinted with permission from Springer, Copyright 2009.³⁷ 15

Figure 6. TEM micrographs displaying A) 100nm DMPC vesicles - x60K magnification B) 100nm DMPC Vesicles + Gramicidin A - x60K magnification C) 100nm DMPC Vesicles + Gramicidin A - x200K magnification. Ordered structures present in 100nm DMPC lipid vesicles (Panel A) are not disrupted upon incorporation of Gramicidin A in Panels B and C (15:1 DMPC:GA 100nm vesicles). All samples were spotted from 1.0 mg/mL lipid solutions in water for analysis on 400 mesh Formvar carbon TEM grids. Samples were negatively stained using 2% uranyl acetate. Images were acquired on a JEOL 1200EX TEM.. 19

Figure 7. VCFD (vesicle capture-freeze drying) preparation scheme. Samples are prepared such that hydrophobic GA molecules are entrapped in the lipid bilayer formed upon extrusion of lipid/GA solutions through a polycarbonate filter. Vesicle samples with GA present are freeze-dried to remove water and further analyzed by ESI-IM-MS upon resuspension in isobutanol..... 22

Figure 8. Collision Cross Section profile of Gramicidin A $[2M + 2Na]^{2+}$ ions (m/z 1904) electrosprayed from: (A) isobutanol, (B) Non-extruded DPPC lipid and (C) 100nm DPPC lipid vesicles prepared using VCFD. Increased abundance of SSHH conformer (725 \AA^2) of *ca.* 40% peak amplitude is evident upon incorporation of GA into a lipid vesicle using VCFD methodology. 28

Figure 9. CCS profiles of GA $[2M + 2Na]^{2+}$ ions electrosprayed from 100-nm lipid vesicles formed using: (A) DLPC (B) DMPC (C) POPC (D) DEPC lipids. GA conformer heterogeneity decreases as the lipid acyl chain length increases (A-D). Note also that the abundances of the SSHH dimer (725 \AA^2) varies considerably but is highest for the unsaturated acyl chain lipid (POPC). In the case of DEPC, the longest acyl chain lipid, only the antiparallel B-helix conformer is detected..... 31

Figure 10. CCS profiles for deformedylated GA (DGA) $[2\text{DGA} + 2\text{Na}]^{2+}$ and hetero-dimer GA $[\text{GA} + \text{DGA} + 2\text{Na}]^{2+}$ ions. (A) $5\mu\text{M}$ DGA electrospayed from isobutanol. (B) – (D) DGA incorporated into 100-nm DLPC (12:0 PC), POPC (16:0, 18:1 PC) and DEPC (22:1 PC) vesicles, respectively. PDH (668 \AA^2) conformers dominate in all DGA samples indicating a preference for parallel conformers once associated with the bilayer of lipid vesicles. (E) $5\mu\text{M}$ hetero-dimer GA/DGA electrospayed from isobutanol. (F) – (H) hetero-dimer GA/DGA incorporated into 100nm DLPC, POPC and DEPC vesicles, respectively. Hetero-dimer GA associated with lipid vesicles was observed to have low abundance of PDH, and ADH dimers dominate indicating very different conformer preferences for homo- and hetero-dimer ions. 32

Figure 11. Experimental schematic for ESI-IM-MS analysis of gramicidin A (GA) loaded bilayers. VCFD preparation is employed to analyze the effect of altering the physicochemical interactions in the bilayer on the conformational preferences of GA dimers. Depicted are bilayers without cholesterol (left) and with cholesterol (right). Perturbing the physicochemical interactions in the bilayer yields significantly different conformer preferences. 42

Figure 12. CCS profiles for $[2\text{GA} + 2\text{Na}]^{2+}$ ions electrospayed from 100 nm DLPC (A), DPPC (B), POPC (C), DEPC (D), and DSPC (E-F) vesicles containing 0-40 mol% cholesterol (vertical, shown at right) plotted as relative abundance vs. CCS (\AA^2). Acyl chain designations, lipid bilayer thickness (D_B), and gel-to-liquid phase transition temperatures (T_M) are provided for each lipid. Vesicle samples were incubated above their T_M , and DSPC was incubated at $4 \text{ }^\circ\text{C}$ (E) and $60 \text{ }^\circ\text{C}$ (F). Conformers have been labeled according to the following scheme: Purple – Nascent conformer (660 \AA^2), Orange – PDH (675 \AA^2), Green, Magenta – ADH (700 \AA^2), Blue – SSHH (725 \AA^2). 46

Figure 13. CCS profiles for $[2\text{GA} + 2\text{Na}]^{2+}$ ions electrospayed from 100 nm POPC vesicles plotted as relative abundance vs. CCS (\AA^2).

Panels A and B display identical data obtained on a Synapt G2 (R ~25) fit using n = 3 peak fits (Panel A) and n = 4 peak fits (Panel B). Panel C displays high-resolution data obtained on a prototype Bruker TIMS instrument with R>100. Note the magenta nascent peak revealed under the ADH distribution using n = 4 peak-fits in Panel B and the high-resolution TIMS instrument. Molecular dynamics (MD) simulations were performed previously to generate candidate structures for each population, and the two most populated structures for each conformer are shown at top right..... 51

Figure 14. Collision Cross Section profiles for $[2GA + 2Na]^{2+}$ ions electrosprayed from 100 nm DSPC vesicles containing 0, 10 or 40% cholesterol are plotted as relative abundance vs. CCS (\AA^2). Samples were incubated at 60 °C for 24, 48, and 72 h (Figure 14A, 14B, and 14C, respectively). At all incubation times, SSHH (shown in blue) abundance increases when 40% cholesterol is present..... 53

Figure 15. ESI coupled to the mixing tee setup reduces sample preparation time by *ca.* 50% compared to VCFD methodology. GA conformer preferences are obtained directly from lipid bilayers suspended in aqueous solution (solution #1) combined with isobutanol (solution #2). 67

Figure 16. Panel A: ESI mass spectrum for $[2GA + 2Na]^{2+}$ ions electrosprayed from an aqueous solution containing GA inserted in 100nm POPC vesicles. Panels B and C: GA dimer ions analyzed from 100nm vesicles of POPC and DEPC, respectively, using MT-ESI. Note the lack of GA signals in Panel A as a result of the extremely low solubility of GA in aqueous solution..... 69

Figure 17. Collision Cross Section (CCS) profiles for $[2GA + 2Na]^{2+}$ ions electrosprayed from 100nm POPC (A,C) and DEPC (B,D) vesicles. Panels A and B were acquired using Vesicle Capture - Freeze Drying (VCFD) methodology. Profiles in C and D were acquired using MT-ESI of solutions containing aqueous vesicle solutions and isobutanol. Conformers have been labeled

according to the following scheme: orange, PDH (675 Å²); green, ADH (700 Å²); blue, SSHH (725 Å²)..... 70

Figure 18. Collision Cross Section (CCS) profiles for GA mutant dimer ions. Shown at left are data for [2GA3K + 2Na]²⁺ ions electrosprayed from isobutanol (A) and 100nm POPC/POPG (16:0, 18:1 PC/PG) vesicles incubated for either 10.0 min or 24 h (B and C, respectively). Shown at right are CCS profiles for [2GA3K(ipr) + 2Na]²⁺ ions electrosprayed from isobutanol (D) and 100nm POPC/POPG (16:0, 18:1 PC/PG) vesicles incubated for either 10.0 min or 24 h (E and F, respectively). Lysine headgroups on GA3K(ipr) have been modified to include single isopropyl (ipr) groups. GA mutants incorporating lysine were observed to adopt ADH conformers for both the modified and unmodified amine headgroup variants. Conformers have been labeled according to the following scheme: purple, compact conformation (635 Å²); orange, PDH (675 Å²); green, ADH (700 Å²); blue, SSHH (725 Å²)..... 73

Figure 19. Structural depictions of GA3K dimers. Shown in blue / magenta are GA monomers containing Leu to Lys modifications. Sidechains for Lys and Trp residues are shown in red and black, respectively. 75

Figure 20. Collision Cross Section (CCS) profiles for [2GA3K + 2Na]²⁺ (A) and [2GA3K(ipr) + 2Na]²⁺ (B) ions electrosprayed from 100 nm DLPC/DLPG (12:0 PC/PG) vesicles incubated for 10.0 min. Profiles were acquired using the mixing tee apparatus containing aqueous vesicle solutions and isobutanol. Nascent conformers are observed from DLPC bilayers in both modified (ipr containing) and unmodified GA3K dimers. Conformers have been labeled according to the following scheme: purple, nascent conformation (660 Å²); orange, PDH (675 Å²); green, ADH (700 Å²); blue, SSHH (725 Å²). 76

CHAPTER I

INTRODUCTION

Ionization and gas-phase analysis of hydrophobic biological molecules from native-like aqueous solutions proposes a key challenge to the field of mass spectrometry (MS). Developments in the fields of MS, cell biology, and biophysics have recently provided an unprecedented view into cellular processes. Approximately 115,000 protein structures are registered in the RCSB Protein Database, however only around 2000 structures are attributed to membrane proteins. This deficiency in representation masks the importance that understanding the structure of membrane proteins can provide to the development of treatments for a variety of diseases associated with dysfunctional protein structures. Ion channels represent only a subset of the membrane protein family, however deficiencies in the structure of these channels represent an alarming and ever growing portion of the diseases observed in the world population. Ion channel dysfunction is linked to several major diseases such as epilepsy, cystic fibrosis, osteoporosis, and even insulin deficiencies.¹ Over 250 million people worldwide are afflicted with epilepsy, osteoporosis, and cystic fibrosis underscoring the necessity for the development of treatments for these diseases.²⁻⁴ There exists a necessity for developing more powerful tools for biophysical characterization to understand the structure and mechanics of ion channels and membrane proteins in general.

The Utility of Mass Spectrometry in GA Characterization

Since the initial cloning of the KcsA potassium-specific ion channel from *Drosophila Shaker* genes the fields of molecular biology, biochemistry and analytical chemistry have produced collaborative efforts to characterize these complexes.⁵ Through understanding the mechanisms and structure of simple ion channels such as the Gramicidin A dimer complex, insight can be obtained into the mechanics of the more complicated aforementioned diseases.⁶⁻⁷ It is hypothesized that Ion Mobility-Mass Spectrometry (IM-MS) can afford access to structural information of peptide or protein ions produced from an environment that mimics their native state (specifically that of the membrane environment) as the molecules transition to the gas-phase. Combining IM-MS with Electrospray Ionization (ESI) allows for the introduction of a solution-phase peptide or protein in a lipid environment into the mass spectrometer.⁸ It is hypothesized herein that morphological changes in the Gramicidin A dimer complex may be monitored via IM-MS to detect how the gas-phase structure is affected by incorporation into various lipid environments.

Native Structure in Mass Spectrometry

Low solubility in aqueous solution influences some biomolecules to enter into a low dielectric membrane environment i.e. the cell membrane. Heck *et al.* demonstrated that it is possible to introduce cell-membrane mimicking lipid vesicles with hydrophobic peptides inserted into a mass spectrometer to sample only their membrane bound state owing to very low ionization efficiency in aqueous solution of the analyte.⁹ Ion mobility coupled to mass spectrometry (IM-MS) affords the ability to separate ions on the basis of

mass-to-charge ratio (m/z) as well as their respective gas-phase conformations. IM-MS is rapidly evolving as a major tool for structural biology studies, but there remain questions regarding the relationship between structure(s) (conformations) of solution-phase and gas phase biomolecule ions. Thus the question raised by Brueker and McLafferty remains elusive - “for how long, under what conditions, and to what extent, can solution structure be retained without solvent?”¹⁰ Silveira *et al.* has shown that electrospray ionization (ESI) can be used to “trap” native states of peptides/proteins, and these results raise the question of whether membrane bound states of peptides can be trapped in a similar manner.¹¹⁻¹⁴ Similarly, Chen has shown that the tuning conditions under which the analyte is analyzed contribute significantly to the ultimate conformation of the peptide or protein reported by the mass spectrometer during IM separation.¹⁵ We describe in this thesis an ESI-IM-MS approach that preserves the membrane bound structure of the dimerized channel-forming peptide, Gramicidin A, as it transitions inside of model lipid vesicles from solution- to the gas-phase.

Multiple conformations for both the GA monomer and dimer have been explored by various means such as single channel conductance across a bilayer fluorescence measurements and circular dichroism.¹⁶⁻¹⁸ Surprisingly there have been no attempts to investigate GA conformers in lipid membranes via IM-MS although much debate has occurred in the field over the preferred conformation of GA in lipid environments. Since 1960 there have been three conformers proposed for GA dimers as shown in Figure 1. GA adopts beta helix type structures owing to alternating D and L amino acids contained in its primary sequence. This alternation in stereochemistry results in a beta helix with

sidechains protruding exterior to the helix. Owing to the capped N and C termini of GA as well as the exterior sidechain protrusion GA is extremely hydrophobic. The interior of the beta helix structures are lined with polar carbonyl groups from the peptide backbone which aid in the solvation of monovalent cations in their journey through the channel. It is understood that the single stranded head-to-head (SSHH) conformer is the channel active conformation of GA while the antiparallel double helix (ADH) and parallel double helix (PDH) are referred to as pore-like forms. We hypothesize that by utilizing IM-MS the preferred gas-phase conformations of Gramicidin A dimers can be elucidated in an effort to produce biophysically relevant comparisons to solution-phase studies.

Membrane Description

Arguably the most complex (and thus most attractive for structural studies) of environments that peptides exist within is that of the cell membrane. Comprised of lipids, chains of nonpolar carbon arrangements connected to polar headgroup moieties, these cell membranes regulate innumerable processes in the body of eukaryotic organisms. Often times cell membranes are disrupted by the binding events of membrane active peptides or proteins which can allow for insertion of drug molecules or egress of molecules such as dyes.¹⁹⁻²³ Lipid molecules orient themselves in the lipid bilayer in a tail-to-tail arrangement that partitions hydrophobic acyl chains of the lipid inside the solvent-free bilayer interior. A simple arrangement of phospholipid molecules in water will form a spherical mass known as a micelle with all lipid headgroups facing outwards and each tail

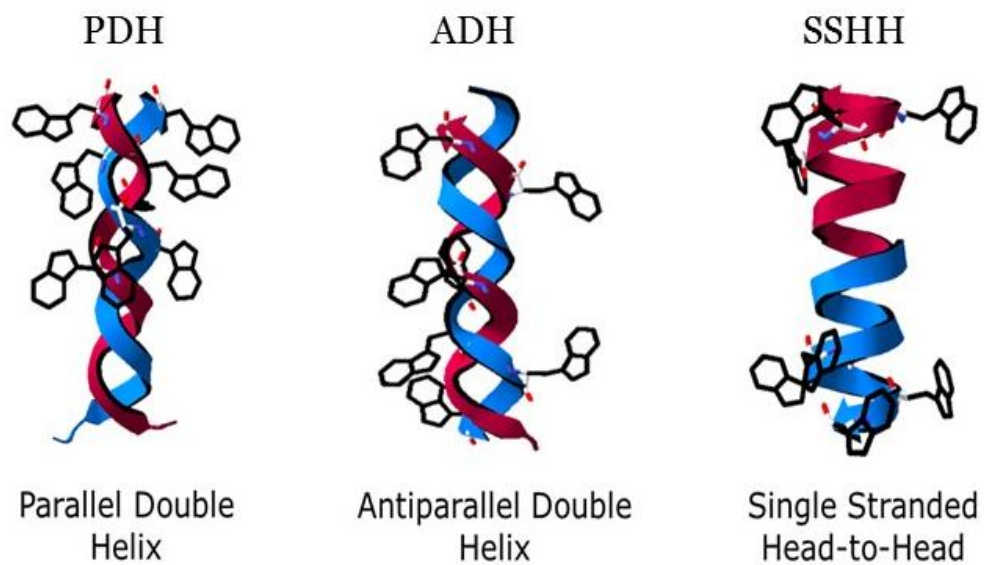


FIGURE 1. Illustrations of three GA conformer families. Tryptophan sidechains at positions 9,11,13 and 15 are denoted in black.

pointing towards the center of the sphere. More typically a multilamellar (or many layered) vesicle forms in which there are many layers of lipids (pointed tail-to-tail) layered on top of each other and separated by an aqueous layer. Freezing and thawing of these multilamellar vesicles will shear outer lipid layers through ice formation and compress the inner layers into one tail to tail arranged bilayer known as a unilamellar lipid vesicle. Forcing unilamellar vesicles through a small pore (typically polycarbonate plastic films with a known pore size) results in a uniformly sized lipid vesicle bilayer with relatively narrow size distribution that can be used for modeling physiological lipid membranes. The flexible hydrophobic “core” of a lipid bilayer serves as an attractive environment for biomolecules that contain a hydrophobic “membrane spanning” segment and acts as a cell mimetic environment with size and composition that can be tailored to suit specific interests.

The membrane active portions of a peptide or protein are most commonly buried within the hydrophobic core of a lipid vesicle bilayer. The nonpolar nature of the bilayer core promotes adoption of a helical conformation of peptides and proteins to minimize interaction of hydrophobic residues (Ala, Gly, Val, Leu, Phe, etc.) from contacting polar water or solvent molecules. While the peptides may also orient themselves towards this helical conformer in non-polar solvents, non-polar solvents are typically unsuitable for MS analysis due to their lack of a protic site making analyte ionization difficult or impossible. Additionally, studies on peptides or proteins from a native membrane environment are more attractive than those from solution alone. Relatively little external solvent exists inside the bilayer allowing maximum free energy gain of the peptide in its

transition from an unfavorable aqueous environment to a bilayer core or, in our case, the gas-phase which exhibits a dielectric constant ($k=1$) mimicking the membrane environment's low dielectric of $\sim 10-20$ (comparable to that of octanol with $k=10-20$).²⁴ Upon analysis of the sequence of GA it can be observed that the C-terminus is rich in Trp residues. Trp residues act as amphipathic anchors that reside at the interface of the hydrophilic and hydrophobic membrane portions.²⁵ Two reasons are provided for the attraction of Trp to the interface: 1) The indole N-H moiety of Trp can hydrogen bond with the oxygen rich phosphate group from the phosphatidylcholine bilayer lipids and 2) π - π interactions or π -cation interactions can occur between the Trp indole ring and phosphate carbonyls / choline moieties. It is also evident that Trp residues have the largest non-polar accessible surface area due to the planar rings making up the indole. Partitioning the hydrophobic rings into the nonpolar hydrocarbon region of the membrane while keeping the N-H moiety available for hydrogen bonding allows the Trp residue to perform as an amphiphilic residue and is believed to influence the anchoring of transmembrane peptides at the bilayer – solvent interface.²⁶ We hypothesize that IM-MS can be used to interrogate the conformational preferences of GA complexes interacting with lipid bilayers to understand the influence that lipid environments exert on membrane protein complexes.

It is the goal of this project to use ion mobility coupled to mass spectrometry to study how insertion of a peptide into a lipid bilayer affects the peptide structure in the gas phase. Lipid vesicles are utilized as model membrane systems to enable observations to be made about this complex system. Conformational shifts in Gramicidin A dimer

preferences that occur upon incorporation into lipid bilayers will be explored in greater detail in this work. We hypothesize that through manipulation of the lipid environment surrounding GA it is possible to influence Gramicidin A dimer conformational preferences. A multitude of routes remain open in regards to studying these transmembrane complexes utilizing IM-MS and lipid systems in order to discern their gas-phase structures. Work has been undertaken to determine how changes in solvent, lipid composition and peptide modifications affect the Gramicidin A structure both in solution and in a cell-like environment in order to obtain information about the underlying processes that govern ion channel function.

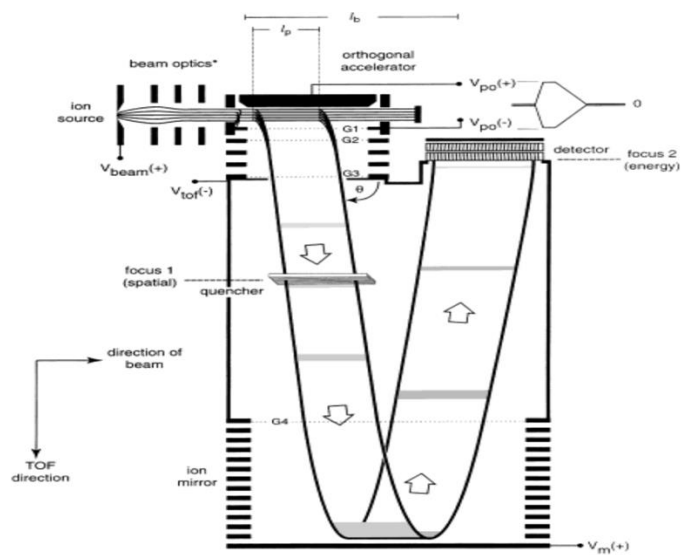


FIGURE 2. Main components and layout of a typical TOF system with reflecting mass analyzer. The ion beam enters from a source at the left and is accelerated to enter the orthogonal accelerator (oa). The beam “fills” the first stage of the oa until a bipolar pushout pulse pair is applied. A packet of ions of length l_p is thus sampled and accelerated through grids to enter the drift region at a potential of V_{tof} . Reflecting TOF optics are used to bring the ions to a space-time focus on the detector. Reprinted with permission from Elsevier, Copyright 1993.²⁷

CHAPTER II

METHODS

Mass spectrometry (MS) provides a facile method for analyzing small volumes of an analyte on short timescales. MS allows for the separation of ions based on their mass to charge (m/z) ratio significantly reducing spectral complexity and allowing for confident assignments of sample signals. While the sample of interest is consumed during mass spectrometric analysis one key advantage is that analyte concentrations can be much lower than that required by NMR based studies – on the order of pico- or femtomoles of analyte per microliter of sample. Spectral complexity is many orders of magnitude less difficult to interpret than is an NMR spectra of the same sample owing to the dispersion of analyte signal based on its m/z .

In all experiments reported herein mass detection is performed using Time of Flight (TOF) techniques wherein ions are injected orthogonally into a time of flight mass detector and converted to m/z values. Figure 2 depicts a typical reflectron TOF setup wherein ions enter from the ion source at left, undergo orthogonal pulsing into the TOF device, and are subsequently analyzed using a multichannel plate (MCP) detector.²⁷ In an orthogonal reflectron TOF ions of varying kinetic energy and mass are injected into the TOF orthogonally to average out the kinetic energy of the ions.

Sample introduction to the instrument is accomplished using electrospray ionization (ESI). ESI is a gentle ionization technique that affords the ability to analyze solution phase peptides or proteins from their native state.²⁸⁻³² The utilization of ESI has increased since it became prevalent in the 1990's and has become the technique of choice

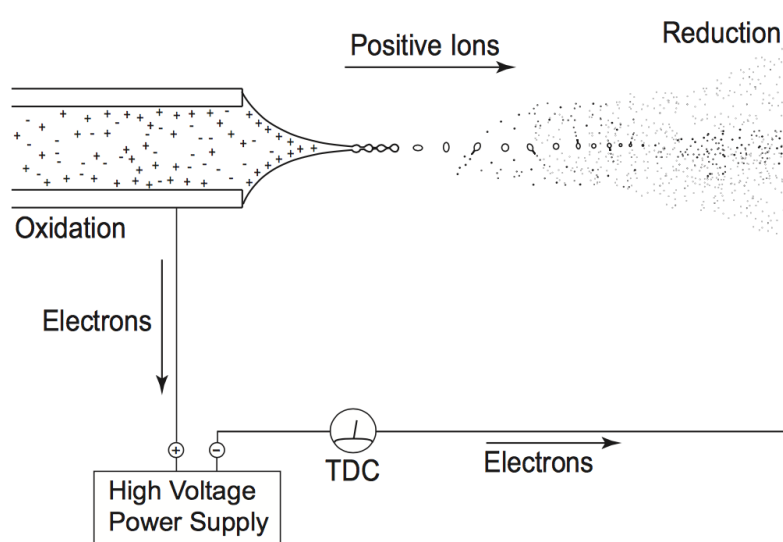


FIGURE 3. Illustration of major processes in an ESI ion source run in the positive ion mode. An electric field penetrates into the liquid leading to an enrichment of positive ions present. Evaporation of the droplets brings the charges closer together. The increasing Coulombic repulsion destabilizes the droplets which emit jets of charged progeny droplets eventually forming free gas-phase ions. Reprinted with permission from Wiley Periodicals, Copyright 2009.³³

for MS analysis of both soluble and insoluble biomolecules. Key developments in the utilization of ESI were the introduction of nano-ESI wherein an emitter can be employed with a reduced diameter opening that yields smaller droplets containing analyte.³⁴⁻³⁵ These smaller droplets require less solvent time for the evaporation of solvent allowing analytes to transition into the gas more more efficiently and with reduced charge yielding more native-like structures for peptides and proteins. Figure 3 depicts a typical nano-ESI setup wherein ions are generated in the positive mode *i.e.* carrying positive charge.³³

ESI affords the ability to perform mass spectrometric analysis on peptides and proteins in their native-like conformations to allow comparisons to be made to their conformations in-vivo. Of great interest is the use of ion mobility (IM) to obtain information about the cross sectional area of a target molecule. Information on the size of an analyte ion is possible through careful measurements of the time taken for an ion to traverse a drift cell filled with a bath gas, Nitrogen or Helium, of known number density. This cell may possess several arrangements; the simplest setup contains ring electrodes defining an ion's flight path as shown in Figure 4.³⁶ A linear electric field applied along the length of the drift tube promotes ion movement towards the detector. This model relies solely on Time of Flight (TOF) much like in mass analysis. Here, a larger molecule such as a protein undergoes more bath gas collisions than a small molecule thus taking longer to traverse the drift cell length. Differences in ion molecular dimensions produce differences in the TOF observed producing what is commonly referred to as an Arrival Time Distribution (ATD) chromatogram. Plotting the ATD vs. the m/z ratios for each time point allows a 2D plot to be prepared with data for similar charge states falling on

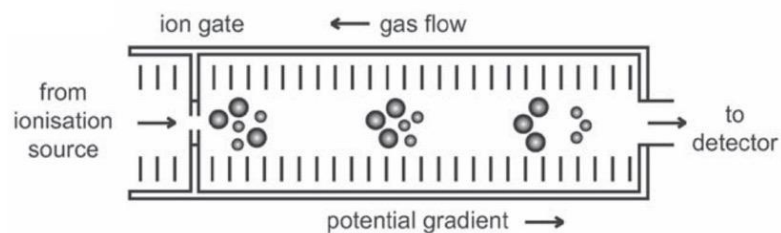


FIGURE 4. Drift tube IM: In drift tube ion mobility, packets of ions traverse the cell along a potential gradient against a constant gas flow. Larger ions experience more collisions with the gas and therefore are retarded relative to smaller ions with a higher mobility. Reprinted with permission from Royal Society of Chemistry, Copyright 2001.³⁶

trendlines as demonstrated in Figure 5.³⁷ Separation of the charge states of an analyte into trendlines allows information to be selected based on areas of interest in the 2D plot – either from ATD or m/z regions. Figure 5 demonstrates the vast conformation space available using IM-MS. Ions of different molecular class can be separated based on their Collision Cross Section (CCS) values to distinguish between isobaric species during analysis. Native membrane peptide/protein analysis typically requires ESI analysis of samples of the analyte inserted into a lipid environment. Using IM-MS it is possible to isolate the protein analyte signal using 2D data selection in order to remove interference from abundant lipid signal. Ionization of the analyte is often difficult owing to the nonpolar nature of many membrane peptides and proteins. Peptide or protein signal is often overwhelmed by easily ionized lipid molecules. Using IM-MS greatly reduces the spectral complexity of a sample and allows for the facile separation of biomolecule signal during post-processing data analysis.

CCS values can be obtained directly when utilizing a uniform field drift tube however, the Synapt G2 instrument employed in the studies in the experiments herein utilizes a unique waveform to guide ions through the drift region that requires the creation of a calibration plot to determine CCS values.³⁸ Comparisons are made between the ATD values of a standard analyte observed on the G2 instrument against known values observed on a uniform field instrument to produce comparable CCS values. CCS calibration on the Synapt G2 is described in further detail in Chapters III, IV, and V.

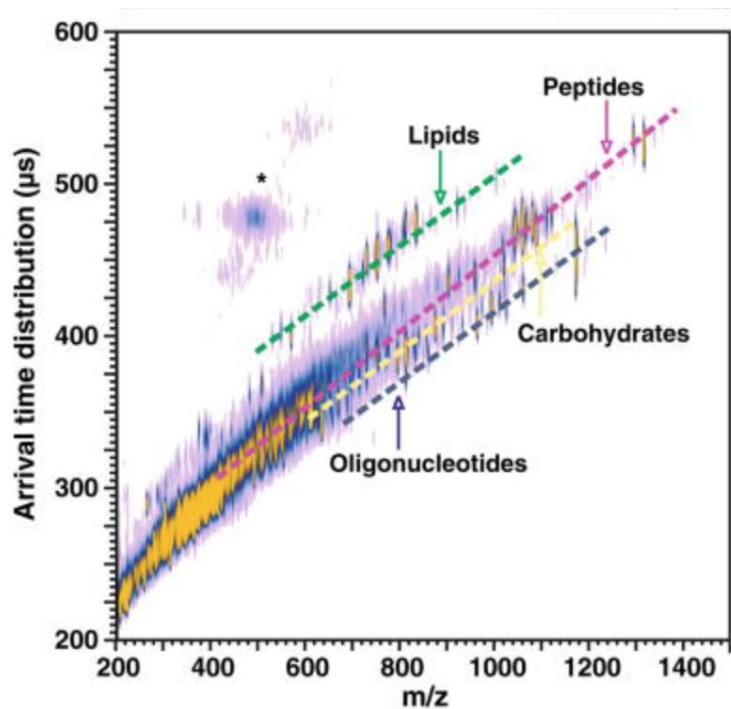


FIGURE 5. A plot of IM-MS conformation space obtained for a mixture of model species representing each molecular class (ranging from seven to 17 model species for each class, spanning a range of masses up to 1,500 Da). Dashed lines are for visualization purposes of where each molecular class occurs in conformation space. Signals in the vicinity of the asterisk arise from limited post-IM fragmentation of the parent ion species. Reprinted with permission from Springer, Copyright 2009.³⁷

Comparable Techniques to ESI

Investigations of membrane-associated peptides and proteins have traditionally been performed using techniques such Nuclear Magnetic Resonance (NMR), Förster Resonance Electron Transfer (FRET), Cryogenic Electron Microscopy (Cryo-EM), and X-Ray Diffraction (XRD).³⁸⁻⁴¹ NMR and XRD have been used most extensively as the methods of choice to elucidate membrane peptide or protein structure. NMR, a typically solution-phase technique, allows for determination of connectivity and spacing of the magnetically susceptible nuclei of a membrane peptide or protein. NMR requires a substantial amount of analyte in order to collect spectra, often on a long timescale (especially if analysis of C¹³ or low abundance isotope nuclei are to be analyzed as this necessitates enrichment of a particular isotope) in relation to MS. While the sample is not destroyed the costs associated with purchasing such a vast amount of sample are high and often expressing milligram-scale quantities of membrane proteins is an arduous task. Spectral complexity is a prominent issue owing to the inherently vast amount of responsive nuclei in a molecule such as a peptide or protein resulting in time consuming analysis. XRD possesses difficulties owing to the challenge of crystallization of a biomolecule such as a protein as this process is difficult in even the best cases. Oftentimes crystallization is near impossible and can take many months to years to obtain an adequate sample (from 6 weeks to 6 months for certain Gramicidin A samples).⁴² Some molecules, such as small transmembrane peptides, are unable to be crystallized and thus are not possible to be analyzed by XRD. A substantial amount of a protein, oftentimes in very short supply, is required in order to adequately initiate the crystallization process.

Compounding the issue is the rather long analysis time of a single crystal which can take anywhere from hours to day(s) on what may not be a single, solvent-free crystal. Extrapolating this effect to larger systems that only remain assembled inside a lipid membrane highlights the importance of new techniques to analyze these systems.

Lipid Vesicle Preparation

The ability to prepare uniformly sized small unilamellar vesicles (SUV) is vital to the ability to interrogate GA conformer preferences across a range of phospholipid bilayer types. First, suspensions of phospholipids and GA are dissolved in chloroform to ensure complete mixing of the peptide and lipid components. This mixture is dried under a stream of nitrogen gas to remove the chloroform and is then placed under vacuum for 4 h to complete the removal of any residual solvent. The sample can then be hydrated using water to initiate swelling of the dried lipid and GA into multilayered films. Sonication of the sample for 30 minutes disrupts the layers and promotes transfer of the lipids into solution. During this step, the swelled layers transition into multilayered vesicles wherein several layers of lipid bilayers, with phospholipids arranged in a tail-to-tail fashion, are separated by aqueous regions. After sonication, the sample is subjected to 8 – 10 cycles of freezing and thawing using liquid nitrogen and a water bath warmed to an appropriate temperature. Freezing of the samples drives the formation of ice crystals in between lipid layers in the multilamellar vesicle and ultimately leads to shearing of the exterior lipid layers. Finally, the sample is passed through a polycarbonate filter containing 0.1 μM pores to ensure a size distribution centered around 100 nm. The lipid vesicle bilayers

produced are typically stable at room temperature however for all work described the vesicles are analyzed immediately unless otherwise noted.

Vesicle Imaging

Figure 6 shows TEM micrographs displaying A) 100nm DMPC vesicles at 60K magnification, B) 100nm DMPC vesicles containing Gramicidin A at 60K magnification, and C) 100nm DMPC Vesicles containing Gramicidin A at 200K magnification. Ordered structures present in 100nm DMPC lipid vesicles (Panel A) are not disrupted upon incorporation of Gramicidin A in Panels B and C (15:1 DMPC:GA 100nm vesicles). Open spherical structures represent vesicles that have ruptured as a result of dehydration during sample deposition. All samples were spotted from 1.0 mg/mL lipid solutions in water for analysis on 400 mesh Formvar carbon TEM grids. Samples were negatively stained using 2.0 % uranyl acetate. Images were acquired on a JEOL 1200EX TEM. Further discussion is provided in Chapter III.

Vesicle Capture – Freeze Drying

Samples of lipid vesicles are prepared for ESI analysis using vesicle capture – freeze drying (VCFD) preparation. Samples of lipid vesicles containing GA are placed into 20 mL glass dram vials and submerged into liquid nitrogen for several minutes to ensure complete freezing of the sample. Upon freezing these samples are subsequently placed into a vacuum desiccator to allow for sublimation to occur. Samples must be left to freeze-dry for *ca.* 12 hours. Upon completion of the freeze drying process the GA containing lipid vesicles are dissolved into isobutanol, unless otherwise noted, and immediately analyzed using ESI.

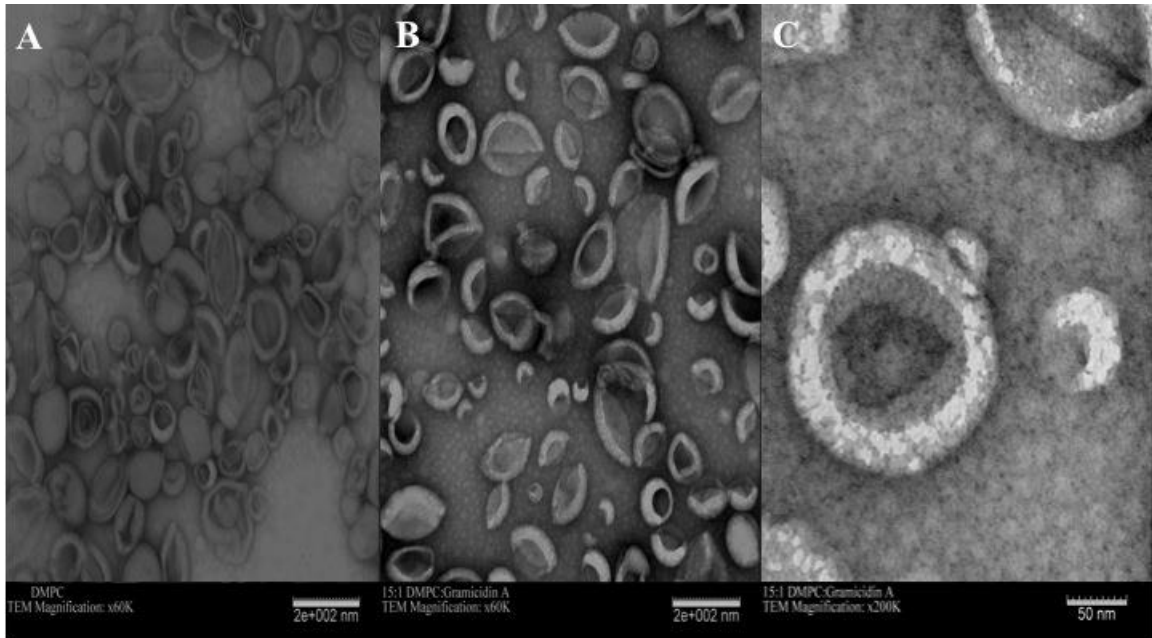


FIGURE 6. TEM micrographs displaying A) 100nm DMPC vesicles - x60K magnification B) 100nm DMPC Vesicles + Gramicidin A - x60K magnification C) 100nm DMPC Vesicles + Gramicidin A – x200K magnification. Ordered structures present in 100nm DMPC lipid vesicles (Panel A) are not disrupted upon incorporation of Gramicidin A in Panels B and C (15:1 DMPC:GA 100nm vesicles). All samples were spotted from 1.0 mg/mL lipid solutions in water for analysis on 400 mesh Formvar carbon TEM grids. Samples were negatively stained using 2% uranyl acetate. Images were acquired on a JEOL 1200EX TEM.

CHAPTER III

ELUCIDATION OF CONFORMER PREFERENCES FOR A HYDROPHOBIC
ANTIMICROBIAL PEPTIDE BY VESICLE CAPTURE-FREEZE DRYING: A
NOVEL PREPARATORY METHOD COUPLED TO ION MOBILITY – MASS
SPECTROMETRY*

Introduction

Channel forming peptides play important roles in a number of antimicrobial biological processes including regulation and selectivity of ion transport across cellular membranes.⁴³⁻⁴⁴ Understanding how peptide structure and the local environment influences the biological activity and conformer preferences of biomolecules is a major challenge for experimental structural biology. Often the active species of many antimicrobial peptides results from the self-assembly or interaction of these molecules with other peptides/proteins and/or lipids.⁴⁵ There are relatively few experimental approaches that can be used to measure conformational heterogeneity, the effects of conformational heterogeneity on bioactivity, or how bioactivities of peptides/proteins are influenced by physico-chemical properties and composition of lipid membrane bilayers. Here, we describe a novel sample preparation method that is compatible with ion mobility-mass spectrometry (IM-MS) for directly measuring the influence of lipid bilayer membranes on conformer preferences and conformer heterogeneity of a membrane

*Reprinted with permission from “Elucidation of conformer preferences for a hydrophobic antimicrobial peptide by vesicle capture-freeze-drying: a preparatory method coupled to ion mobility-mass spectrometry” by Patrick, J.W.; Gamez, R.C.; Russell, D.H., *Anal. Chem.*, 2015, 87, 578-583, Copyright 2015 American Chemical Society.

peptide. This novel sample preparation methodology, termed *vesicle capture-freeze drying* (VCFD), is combined with ESI-IM-MS to preserve the membrane bound structure of the dimerized channel-forming Gramicidin A (GA) as it transitions (inside the bilayer of model lipid vesicles) from solution to the gas-phase (Figure 7). The hydrophobic nature of GA ensures that only membrane-bound conformations are monitored thus overcoming a significant barrier to direct analysis from aqueous solution by mass spectrometry. The VCFD-ESI-IM-MS approach provides new insights about this important biological model of channel forming antimicrobial peptides and lipid bilayer membranes.

Gramicidin A has been extensively studied and is known to form transmembrane ion channels that are selective for monovalent cations, and specific conformations of the self-assembled dimers have been proposed.⁴⁶⁻⁴⁸ The conformer preferences of GA dimers inserted into lipid membrane bilayers and how the physico-chemical properties of the lipid bilayer alter conformer preferences are not fully understood. The membrane activity of GA is attributed to its hydrophobic character, arising from the sequence of alternating D- and L-amino acids that facilitate formation of β -helical conformers by partitioning of hydrophobic side chains to regions exterior to the helix. The very low solubility of GA in water (<500 nM) typically limits structural characterization studies to non-aqueous environments.⁴⁹ Previous NMR studies of GA dimers attempted to circumvent solubility issues by associating the dimer complexes with water soluble micelles; however, this strategy resulted in congested spectra, owing to the dynamic nature of the dimer conformers.⁵⁰⁻⁵² Additionally, crystallographic techniques failed to elucidate GA dimer conformer preferences in lipid bilayer membranes because the formation of these

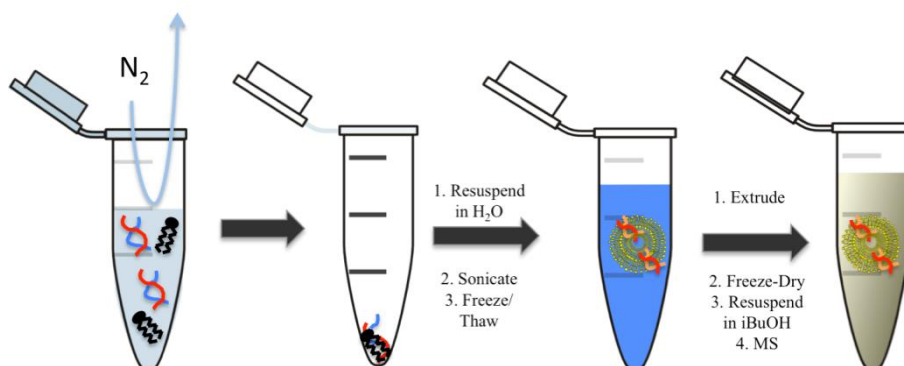


FIGURE 7. VCFD (vesicle capture-freeze drying) preparation scheme. Samples are prepared such that hydrophobic GA molecules are entrapped in the lipid bilayer formed upon extrusion of lipid/GA solutions through a polycarbonate filter. Vesicle samples with GA present are freeze-dried to remove water and further analyzed by ESI-IM-MS upon resuspension in isobutanol.

assemblies requires that the hydrophobic interactions remain intact throughout the analysis.⁵³⁻⁵⁴

The applications of ion mobility (IM) in biophysical chemistry and structural biology have grown considerably in the past decade owing to its ability to separate gas-phase ions on the basis of size-to-charge, yielding measurements of accurate ion-neutral collision cross sections (CCS).⁵⁵⁻⁵⁶ The combination of IM with mass spectrometry (MS), which affords accurate measurements of mass-to-charge ratios (m/z), and molecular dynamics (MD) simulations that can be used to correlate ion CCS with candidate ion conformations, is rapidly evolving as a new tool for the study of complex biological systems.^{10, 57} In earlier papers we used IM-MS to examine the conformer preferences of the GA monomer and to determine the solvent-dependent self-assembly and conformer preferences of the GA dimer. The VCFD approach combined with ESI-IM-MS provides new insights regarding the effects of local environment on the conformer preferences of this important model membrane peptide.

Materials and Methods

Gramicidin A amino acid sequence: HCO-L-Val-Gly-L-Ala-D-Leu-L-Ala-D-Val-L-Val-D-Val-L-Trp-D-Leu-L-Trp-D-Leu-L-Trp-D-Leu-L-Trp-NHCH₂CH₂OH

Materials

Gramicidin A (Sigma-Aldrich St. Louis, MO, USA; $\geq 90\%$ purity) was used as received and dissolved in HPLC grade methanol (Sigma Aldrich St. Louis, MO, USA) at a concentration of 1 mg/mL without further purification. Lipids were received as 10 mg/mL solutions in chloroform (Avanti Polar Lipids, Alabaster, AL) and portioned out

into 500 μ L aliquots containing 5mg of lipid. HPLC grade methanol, ethanol, n-propanol and isobutanol (Sigma-Aldrich St. Louis, MO, USA) were used as received. Deformylated GA was prepared by reacting 1.0 mg/mL GA in methanol with 2.0 M hydrochloric acid for 2 hours followed by lyophilization to yield a dry powder that was used without further purification.

Vesicle Capture-Freeze Drying Method (VCFD)

Samples of lipid dissolved in chloroform, and Gramicidin A dissolved in ethanol, were combined at \approx 50:1 lipid:peptide for experiments detailed in this work, dried under nitrogen gas, and subsequently desiccated under vacuum to remove residual solvent. Samples were rehydrated to 1 mg/mL lipid in 18M Ω distilled water and sonicated for 30 minutes. Ten freeze-thaw cycles were performed on each sample using liquid nitrogen and \sim 50 $^{\circ}$ C water. Samples were then extruded through a size controlled polycarbonate filter (100 nm pore size) to produce uniform vesicles. Vesicle/GA solutions were allowed to equilibrate at 4 $^{\circ}$ C overnight. Prior to ESI, GA samples in vesicles were freeze-dried using liquid nitrogen and a vacuum desiccator. Immediately prior to ESI each lyophilized sample was dissolved in isobutanol for analysis. Control samples were prepared by combining GA and a desired PC lipid in isobutanol followed by sonication for 30 minutes, ten freeze-thaw cycles and subsequent freeze-drying prior to ESI. Figure 6 demonstrates that the incorporation of GA into DMPC lipid vesicles does not disrupt the vesicle structure. Figure 6A represents a control in which 100nm DMPC vesicles were imaged using TEM analysis. Figure 6B and Figure 6C show a DMPC vesicle containing GA at a 15:1 lipid : peptide ratio at either 60K (6B) or 200K (6C) resolution. Figure 6 demonstrates

that no significant disruption to the vesicle shape or size was observed using TEM analysis when GA was incorporated into lipid vesicles prepared using a VCFD approach prior to the freeze-drying portion of the preparation. Samples imaged by TEM were negatively stained prior to TEM analysis using a 2.0 % uranyl acetate solution.

Electrospray – Ion Mobility – Mass Spectrometry (ESI-IM-MS)

All ESI-MS and ESI-IM-MS experiments were carried out on a Waters Synapt G2 HDMS (Waters Corp., Milford, MA, USA) equipped with a nano-ESI source operating at ~100 °C. Spectra were acquired in positive ion mode using a 1.5 – 2 KV voltage applied to the capillary tips. ESI tips were manufactured in-house by a gravity-pulled method using fused silica capillary line. Parameters for the traveling wave ion mobility cell were set at 32V wave height and 400 m/s wave velocity. High resolution GA spectra were acquired on an Agilent 6560 Ion Mobility QTOF LC/MS instrument; see supplemental material.

All analyses were performed using MassLynx v4.1 software. All reported CCS were obtained by using a calibration plot from data acquired with instrument conditions identical to those used to analyze GA samples. CCS values for peptide ions, *i.e.*, $[M + 2H]^{2+}$ ions produced by tryptic digestion of myoglobin and cytochrome C, obtained from the Clemmer database were used as calibrants.⁵⁸⁻⁵⁹ CCS calibration was performed as previously described by Ruotolo.⁶⁰ Although there are discrepancies in CCS values obtained using helium versus nitrogen collision gas, reasonable agreement was observed between calibrated CCS and theoretical CCS values reported previously by Chen *et al.* Williams showed that ion mobility peak profiles and collision cross sections obtained on

the Synapt G2 are sensitive to instrument tuning; however, the experiments described here were all performed using instrument tuning parameters that minimize ion heating.⁶¹

Results and Discussion

Vesicle capture-freeze drying (VCFD) is used to capture the ensemble of water-insoluble peptides that are interacting, either by “carpeting” onto the surface or inserting into the lipid vesicle, with the lipid bilayer membrane. Removal of residual water from GA-entrapped vesicles yields a solvent-free lyophilized peptide that can be resuspended in isobutanol and then analyzed by ESI-MS and ESI-IM-MS. Chen *et al.* previously demonstrated that the rate of disassociation (monomerization) of GA dimer ions, specifically $[2M + 2Na]^{2+}$ ions, is similar to values obtained using circular dichroism, and the rate of monomerization decreases as the alcohol chain length increases.⁶²⁻⁶⁴ Thus, resuspension of lyophilized GA-containing/lipid-vesicles in isobutanol permits ESI under conditions where the kinetic rates of monomerization do not significantly alter the conformer heterogeneity. Previous research investigating peptide/protein complexes has demonstrated that the conformer preferences of these complexes are sensitive to changes in their local environment.⁶⁵ While GA complexes have been extensively studied in solution-phase environments, *viz.* organic solvents, these environments do not accurately represent the physico-chemical interactions GA experiences when associated with a lipid membrane.⁶⁶ The question that must be addressed is, *do GA $[2M + 2Na]^{2+}$ dimers captured by VCFD and then analyzed by ESI-IM-MS retain membrane-bound conformations during transfer from the solution phase to solvent-free gas phase ions?*

Determining the Identity of GA [2M + 2Na]²⁺ Dimer Peaks

CCS profiles for GA [2M + 2Na]²⁺ ions (1904 *m/z*) were obtained by using ESI-IM-MS from solutions of isobutanol. Three dimer conformers have been proposed for GA: (i) a parallel double helix (PDH); (ii) antiparallel double helix (ADH); and (iii) single stranded head-to-head dimer (SSHH). Experimental CCS values and ribbon structures for each of the conformers are contained in Figure 8A. Experimental CCS values for the SSHH dimer (725 Å²) deviate by less than 1% from previously calculated values (728 Å²) reported by Chen and coworkers.⁶⁴ CCS values for PDH and ADH (673 and 697 Å², respectively) are also in excellent agreement (+/- 2.5%) with values reported by Chen. The agreement between experimental CCS values and values calculated from NMR structures

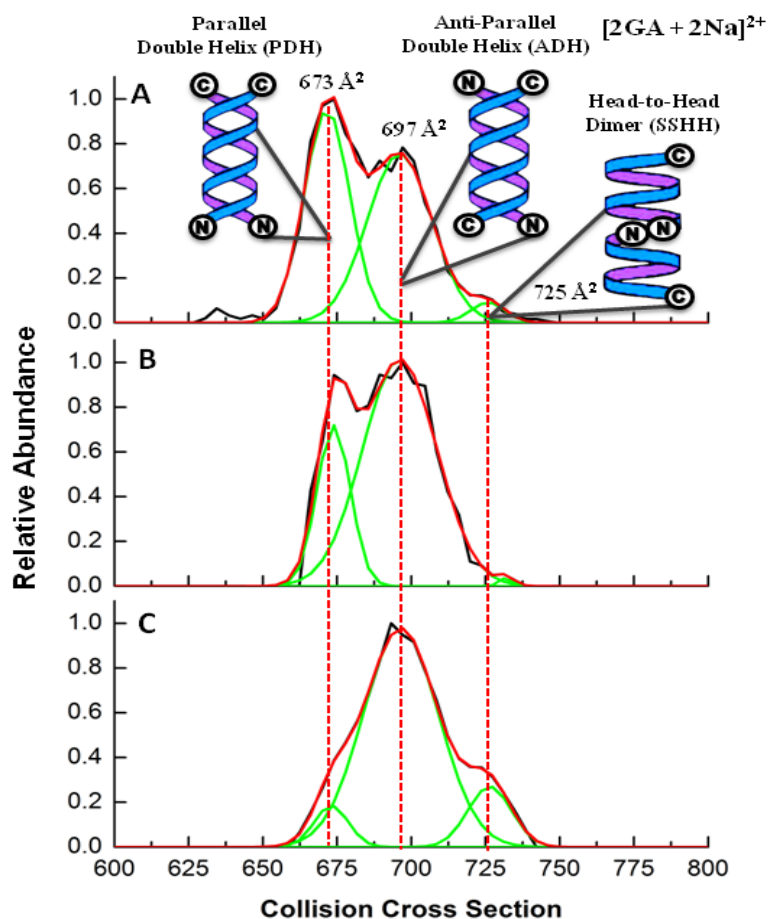


FIGURE 8. Collision Cross Section profile of Gramicidin A $[2M + 2Na]^{2+}$ ions (m/z 1904) electro-sprayed from: (A) isobutanol, (B) Non-extruded DPPC lipid and (C) 100nm DPPC lipid vesicles prepared using VCFD. Increased abundance of SSHH conformer (725\AA^2) of *ca.* 40% peak amplitude is evident upon incorporation of GA into a lipid vesicle using VCFD methodology.

reported by Cross supports the hypothesis that conformers observed by IM-MS in these experiments resemble the three commonly reported solution-phase dimers.⁶²⁻⁶³ This observation is consistent with results reported by Urry and coworkers that showed that the SSHH conformer formed from two left-handed π^6_{LD} single-stranded monomers associated in an N-terminal to N-terminal fashion based on channel conductance measurements and molecular modeling.⁴⁸ The exact mechanism by which these complexes assemble in the low dielectric environments remains unclear despite attempts by Arseniev and Cross to demonstrate the presence of these conformers using NMR and MD simulations.⁶⁷⁻⁷¹

CCS profiles for GA $[2M + 2Na]^{2+}$ ions from vesicles comprised of the phosphatidylcholine DPPC prepared by VCFD are shown in Figure 8. In comparison to a control sample with DPPC dissolved in isobutanol (Figure 8B), an increase in peak amplitude of ~40% is observed for the SSHH conformer at 725 \AA^2 for GA incorporated into DPPC vesicles (Figure 8C). The above results clearly show that the presence of free lipid does not significantly alter the solution phase conformer preferences. CCS profiles for DLPC (12:0 PC), POPC (16:0, 18:1 PC) and DEPC (22:1 PC) control samples prepared identically to the DPPC sample in Figure 8B are provided in Figure A1.

Analysis of Lipid-dependent Conformer Preferences

GA channel behavior is known to be sensitive to changes in membrane thickness, *i.e.*, the hydrophobic mismatch between gramicidin dimers and lipid bilayers.⁷² Acyl chain length and extent of unsaturation has a direct influence on the bilayer fluidity, thickness, and packing efficiency; unsaturated acyl chains increase the fluidity of the bilayer permitting insertion or transport of peptides/proteins across membranes.⁷³⁻⁷⁷ Figure 9

contains CCS profiles for GA dimers for a series of phosphatidylcholine (PC) vesicle bilayers with increasing chain lengths; (A) DLPC, (B) DMPC, (C) POPC and (D) DEPC; the bilayer thickness for A – D spans the range of $\sim 30 \text{ \AA}$ to $\sim 44 \text{ \AA}$.⁷⁸ DLPC vesicles form thinner bilayers and give rise to a higher degree of micro-heterogeneity, and there is a clear preference for the formation of the ADH dimer. The abundances of PDH and SSHH increase as the bilayer thickness increases; however for DEPC a single conformer, ADH, is detected. The observed trend in the conformer heterogeneity supports the notion that thinner bilayers accommodate a variety of GA conformers, whereas a thicker bilayer accommodates a much narrower distribution of conformers. In the case of bilayers with positive hydrophobic mismatch, where GA dimer lengths are equal to or larger in diameter than the bilayer, rearrangement of GA dimers may take place in order to minimize unfavorable interactions with solvent.⁷⁹⁻⁸⁰ The appearance of a fourth conformer centered at $\sim 665 \text{ \AA}^2$ is only observed from DLPC vesicles. It appears that this conformer is favored owing to the positive hydrophobic mismatch of the thin bilayer and comparatively long GA complexes; however this is the only example where a new conformer has been observed. Further experiments are underway to probe the perturbations on GA complexes introduced in bilayers with extreme hydrophobic mismatches.

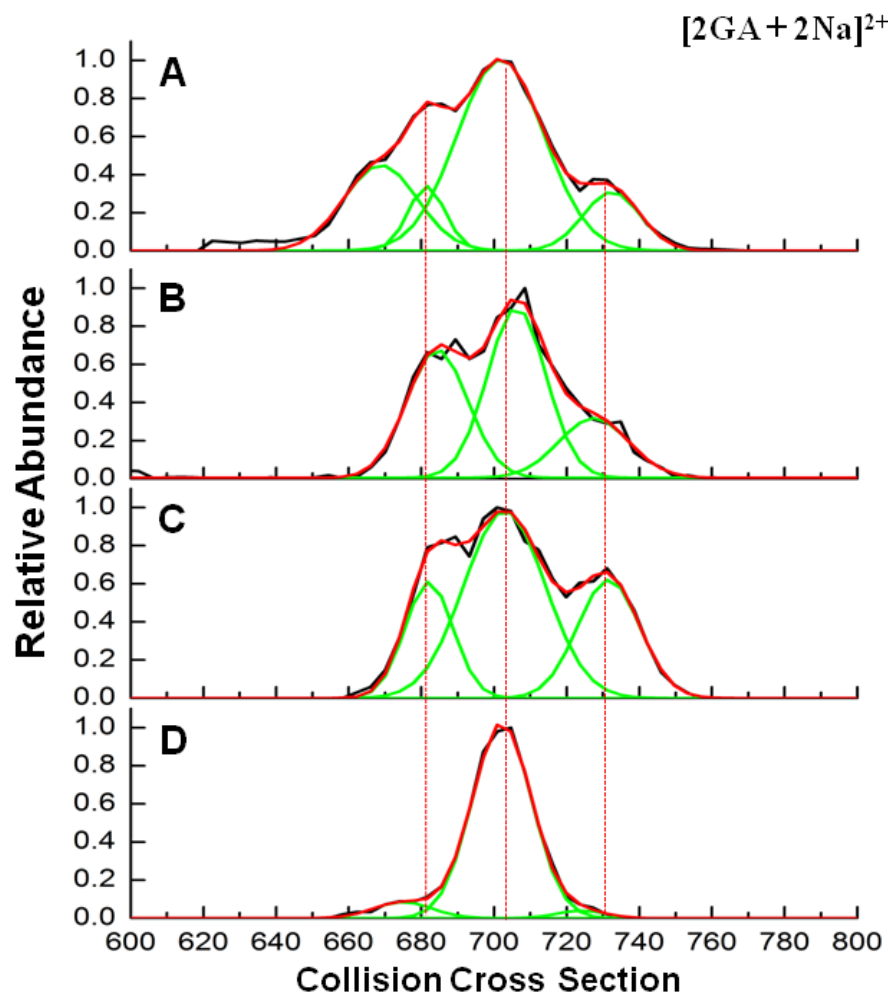


FIGURE 9. CCS profiles of GA $[2M + 2Na]^{2+}$ ions electrospayed from 100-nm lipid vesicles formed using: (A) DLPC (B) DMPC (C) POPC (D) DEPC lipids. GA conformer heterogeneity decreases as the lipid acyl chain length increases (A-D). Note also that the abundances of the SSHH dimer (725 \AA^2) varies considerably but is highest for the unsaturated acyl chain lipid (POPC). In the case of DEPC, the longest acyl chain lipid, only the antiparallel B-helix conformer is detected.

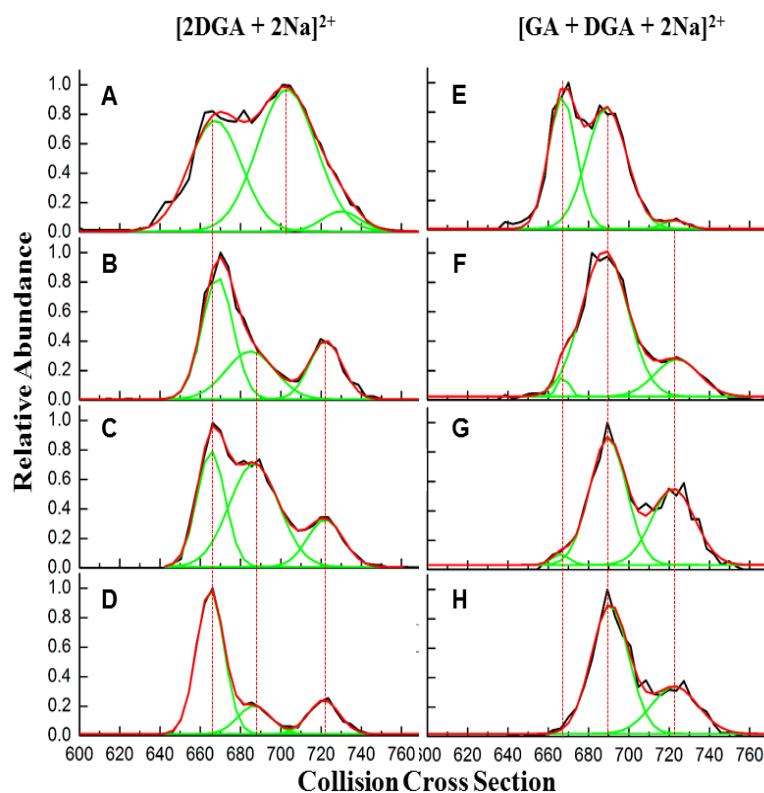


FIGURE 10. CCS profiles for deformedylated GA (DGA) $[2\text{DGA} + 2\text{Na}]^{2+}$ and hetero-dimer GA $[\text{GA} + \text{DGA} + 2\text{Na}]^{2+}$ ions. (A) $5\mu\text{M}$ DGA electro sprayed from isobutanol. (B) – (D) DGA incorporated into 100-nm DLPC (12:0 PC), POPC (16:0, 18:1 PC) and DEPC (22:1 PC) vesicles, respectively. PDH (668 \AA^2) conformers dominate in all DGA samples indicating a preference for parallel conformers once associated with the bilayer of lipid vesicles. (E) $5\mu\text{M}$ hetero-dimer GA/DGA electro sprayed from isobutanol. (F) – (H) hetero-dimer GA/DGA incorporated into 100nm DLPC, POPC and DEPC vesicles, respectively. Hetero-dimer GA associated with lipid vesicles was observed to have low abundance of PDH, and ADH dimers dominate indicating very different conformer preferences for homo- and hetero-dimer ions.

The influence of lipid acyl chain unsaturation on conformer preferences of GA is illustrated by comparing the data for POPC with DLPC, DMPC and DEPC vesicles. POPC vesicles yield the highest abundance of SSHH (725 \AA^2) indicating that a balance between lipid acyl chain length and extent of acyl chain unsaturation must be met. Conversely, increasing the acyl chain length increases the abundance of ADH (697 \AA^2), and for DEPC the ADH dimer is preferred whereas PDH and SSHH conformers are virtually absent. GA is known to employ Trp residues to anchor itself in the lipid headgroup/solvent interface of membranes; in ADH conformers this yields local anchoring at either side of the bilayer owing to Trp residues located on the C termini of GA.⁸¹ Thicker bilayers are known to introduce negative hydrophobic mismatch in which the bilayer “puckers” to accommodate GA dimers with a shorter hydrophobic thickness than the bilayer thickness.⁸²⁻⁸³ This puckering would induce a stretching force longitudinally along the length of the anchored ADH dimer yielding a decreased number of antiparallel conformers as evidenced by the decrease in peak width at 697 \AA^2 . GA dimers may encounter constraints limiting flexibility when a stretching force acts on the complex. The application of this force on a given conformer, in this case ADH, is observed as a decrease in conformational micro-heterogeneity, *i.e.*, narrower peak width using IM-MS. In some cases we observe peak broadening; however, high resolution IM-MS has demonstrated the presence of discrete conformers that are not visible under lower resolution conditions emphasizing the need for increased IM resolving power (Figure A2).

Effects of Deformylation of Gramicidin A on Conformer Preferences

The hydrophobicity of GA is derived from the amino acid sequence and the formyl and ethanolamine protected N- and C-terminus, respectively. This begs the question, *how would the presence of a hydrophilic N-terminus alter interactions with lipid vesicles and conformer preferences?* For example, the hydrophilic N-terminus of the DGA dimer would be expected to favor or possibly be anchored at the bilayer interface. This idea was addressed by measuring the conformer preferences of deformylated GA (DGA) [2DGA + 2Na]²⁺ ions in isobutanol, DLPC, POPC and DEPC vesicles (see Figure 10A-D, respectively). Deformylation increases the equilibrium abundances of the dimer for both ADH and PDH conformers relative to SSHH, but the largest increase is for the PDH dimer. Similar changes in abundances of the dimers are observed for VCFD prepared samples. The most significant shifts occur for DEPC; recall the DEPC native GA (Figure 9D) dimers favor the ADH conformer, whereas DGA (Figure 10D) favors the PDH dimers. These results are consistent with the observation reported previously by de Groot that deformylation shifts the equilibrium between GA conformers toward double helical conformations, *viz.* ADH or PDH populations in lipid bilayer environments.⁸⁴ de Groot suggests that rearrangement of DGA conformers to PDH dimers permits solvation of the hydrophilic N-termini owing to their location at the bilayer interface. The lower abundance for the SSHH dimers in thick DEPC bilayers (Fig. 10D) when compared with DLPC or POPC (Fig. 10B, 10C) vesicles is also consistent with de Groot's hypothesis. Specifically, it may not be feasible for SSHH dimers to span the thicker DEPC bilayer, and rearrangement of the SSHH dimers to PDH dimers affords solvent-induced

stabilization of the N-terminus. In all cases the peak widths for the DGA dimers (Figure 10 B-D) are narrower than those analyzed from isobutanol solutions. The narrower peak widths indicate increased ordering of conformers which is possibly a result of spatial confinement of the DGA dimer complexes within the lipid acyl chains.

Peptide deformylase is known to result in incomplete deformylation *in vivo*, thus native environments are potentially composed of both homo- and hetero-dimers.⁸⁵ The hetero-dimer GA/DGA, prepared *in vitro* by mixing DGA and GA monomers (see Experimental Section), provides a unique system for monitoring the effects of an unprotected N-terminus on the conformer preferences and stability of GA dimer complexes. Figure 10 contains CCS profiles for hetero-dimer $[GA + DGA + 2Na]^{2+}$ ions electrosprayed from isobutanol (10E), and 100 nm vesicles formed from DLPC (F), POPC (G), and DEPC (H). In isobutanol, the homo- and hetero-dimers exhibit similar conformer preferences; however, the VCFD prepared hetero-dimer ions yield very different conformer preferences. The hetero-dimer preferences are markedly different from homo-deformylated dimer, which are dominated by PDH dimers. The hetero-dimer projects a single hydrophilic site at the bilayer interface, potentially interacting with adjacent lipid headgroups and interfacial water molecules thereby stabilizing the GA/DGA complex.

Although the abundances of homo- and hetero-SSHH dimers are quite low in isobutanol solutions, the abundances of both homo- and hetero-SSHH dimers are relatively high in samples prepared by VCFD (Figure 10B-D, F-H). Assuming the SSHH dimers are oriented in a head-to-head fashion this orientation places the hydrophilic N-terminus toward the membrane interior. De Groot suggested that for DGA SSHH

complexes the “electrostatic repulsion between [these] positive charges cause the N termini to fold toward the interior of the channel region, thereby destabilizing [the] helical dimeric structure...” In 2DGA samples we observe lower abundance of SSHH as lipid acyl chain length increases, *i.e.* bilayer thickness increases. If Trp residues are anchoring GA at the bilayer interface, the reduction in SSHH abundance could be indicative of longitudinal stretching occurring along the length of the complex as we proposed for native GA incorporated into DEPC vesicles. According to De Groot, N-terminal hydrophilic sites are folded away from each other in DGA SSHH complexes. However, when lipid acyl chain length is increased, stretching forces may expose the hydrophilic N-termini to the hydrophobic membrane interior. We observe a decrease in the abundance of the homo-dimer SSHH from DEPC vesicles indicating that the complex may be destabilized in accordance with de Groot’s hypothesis. The abundance of SSHH hetero-dimer samples is not altered upon increasing acyl chain length, which indicates that inclusion of a single hydrophilic site can be accommodated without disruption of SSHH dimers. Further studies using a broader range of phosphatidylcholine lipids are underway to determine how changes in lipid bilayer thickness or the extent of acyl chain unsaturation perturbs DGA conformer preferences. Channel-type (SSHH) conformers are observed to form in DGA samples in higher abundance when associated with lipid bilayers in comparison to solution-phase environments despite incurring an entropic penalty by placing two hydrophilic sites in the interior of the bilayer. These future studies of deformed GA may provide new insights into lipid membrane “assembly” effects, *i.e.* the preference for GA to form channel, or channel-like, conformers in lipid bilayers.

Conclusion

The use of ESI for studies of self-assembled hydrophobic peptide dimers poses a unique challenge owing to the loss of the hydrophobic forces driving association during the transition of a biomolecule from the solution phase to a solvent-free, gas-phase ion. The vesicle capture-freeze drying (VCFD) method is compatible with MS and IM-MS and it provides a novel approach to study gas-phase dimer ion conformer distributions of hydrophobic peptide complexes. GA dimer complexes successfully captured by lipid vesicles suspended in aqueous solution were analyzed using the VCFD method to monitor the behavior of dynamic dimers. ESI-IM-MS data show that the gas-phase abundances of each GA $[2M + 2Na]^{2+}$ dimer conformer are (i) affected by incorporation into lipid bilayer membranes as well as solutions containing lipids, and (ii) solution-phase physico-chemical interactions influenced by lipids can be probed by monitoring conformer preferences using IM-MS. Furthermore, changes in acyl chain length and extent of acyl chain unsaturation of the vesicle-forming lipids directly alter the conformer preferences of the $[2M + 2Na]^{2+}$ dimer ions. The VCFD methodology makes possible, for the first time, the direct measure of the gas-phase conformer preferences of lipid bilayer bound GA dimers from an originally aqueous solution using ESI-IM-MS. The results detailed in this report unambiguously demonstrate that the gas-phase conformer distributions sampled by ESI-IM-MS are directly related to the ensemble of conformers observed in the solution phase.

CHAPTER IV
THE INFLUENCE OF LIPID BILAYER PHYSICOCHEMICAL PROPERTIES ON
THE CONFORMER PREFERENCES OF THE MODEL ION CHANNEL
GRAMICIDIN A*

Introduction

Many biological processes including peptide- or protein-lipid interactions are influenced by the identity and localization of the lipids comprising cellular membranes.⁸⁶⁻⁸⁷ Membrane lipids are polymorphic entities owing to their ability to exist in several different states and structures based on a number of external variables such as temperature, pressure, and pH.⁸⁸⁻⁸⁹ It has been hypothesized for many years that changes in the physicochemical interactions in the bilayer can alter the conformer distribution of membrane proteins.⁹⁰⁻⁹¹ Cholesterol, a major component of eukaryotic cellular membranes, serves to assist in modulating the physicochemical properties (fluidity and rigidity of the bilayer) and can also influence the enthalpy of the phase transition in lipid membranes.⁹²⁻⁹³ Understanding the relationship between lipid identity and physicochemical interactions will lead to fundamental insights of the underlying mechanisms of peptide/protein interactions within lipid bilayers. Wimley noted that "...a major bottleneck in the development of new amphipathic membrane peptide drugs arises

*Reprinted with permission from "The Influence of Lipid Bilayer Physicochemical Properties on Gramicidin A Conformer Preferences" by Patrick, J.W.; Gamez, R.C.; Russell, D.H., *Biophys. J.*, 2016, 110, 1826-1835, Copyright 2016 Biophysical Society.

from our inability to describe their mechanism-of-action (MOA) in physical–chemical terms...”.⁹⁴ This view underscores the necessity for an increased understanding of peptide/protein interactions, especially ion-channel formation. Here, phospholipid bilayers are utilized to elucidate the effect of altering lipid bilayer physicochemical properties on the conformer preferences of a well-studied gramicidin ion-channel complex, *viz.* gramicidin A.

There have been numerous reports on conformer preferences of gramicidin A (GA), a 15-residue dimer-forming ion channel. Chen recently reported the kinetics of disassociation and conformer preferences of GA dimers using electrospray ionization–ion mobility–mass spectrometry (ESI-IM-MS), collision-induced dissociation (CID), and hydrogen/deuterium exchange (HDX)-MS.⁶⁴ GA dimer ions, $[2 \text{ GA} + 2 \text{ Na}]^{2+}$, were observed to adopt three distinct dimeric conformers in the gas phase: the parallel double-helix (PDH), antiparallel double-helix (ADH), and single-stranded head-to-head dimer (SSHH). MOBCAL/molecular dynamics (MD) simulations were performed to assign representative structures to experimentally observed conformers. Solvent polarity was found to directly affect the monomerization kinetics and equilibrium abundances of the dimer ions. Consistent with previous solution-based NMR studies by Cross and coworkers, ADH conformers were found to be the thermodynamically preferred species from low dielectric solutions.⁹⁵ HDX and CID measurements revealed a complex of GA monomers with strong intermolecular hydrogen bonds, consistent with the arrangement of known GA conformers. Coupling IM with HDX-CID methodology provided a comprehensive view of GA self-assembly/disassembly in low dielectric solutions.

We recently described a new approach, vesicle capture – freeze drying (VCFD) coupled to ESI-IM-MS, for studies of membrane-captured GA, which showed that the conformer preferences of GA dimers are highly sensitive to the composition of the lipid bilayer.⁹⁶ The conformers of lipid bilayer bound GA dimers were shown to reflect the ensemble of conformers observed in the solution phase; however, changing the identity of the lipids comprising the bilayer resulted in a significant influence on the preferred conformations of GA dimers. Factors such as temperature, sterol incorporation, and incubation time that ultimately influence the physicochemical properties of lipid bilayers have also been reported to alter the channel activity of gramicidin complexes, but GA dimers have widely been reported to be insensitive to changes in acyl chain length of the lipids comprising the bilayer.⁹⁷⁻⁹⁹ While physical properties of the lipids have been examined, the influence of physicochemical interactions on the assemblage of peptide/protein complexes, *i.e.*, GA ion-channels are neither well-characterized nor well-understood.

Lipid bilayers possess an intrinsic phase transition temperature, T_M , above which acyl chain disorder is greatest, resulting in a liquid disordered (L_D) phase. Conversely, below T_M , lipid acyl chains are ordered (gel-like), referred to as the solid ordered (S_O) phase. Cholesterol incorporation of sufficient quantity into lipid bilayers at a temperature below T_M of a given lipid yields an additional liquid ordered phase, L_O .¹⁰⁰ Lipid acyl chains are fully extended in this phase, similar to the S_O phase, yet retain increased lateral mobility. Cholesterol, an amphiphilic sterol, intercalates between the lipid acyl chains on either the inner or outer leaflet of lipid bilayers yielding an increase in bilayer thickness

owing to increased ordering (extension) of acyl chains. The intercalation of cholesterol between lipid molecules, above or below T_M , occupies the interstitial space between lipids and “stiffens” or increases rigidity of the lipid bilayer. The addition of cholesterol to bilayers at temperatures below their T_M is reported to fluidize the bilayer, likely through disruption of the ordered, gel-like network of lipid acyl chains.⁹² The addition of cholesterol above T_M is reported to decrease lateral mobility of the lipids yielding more rigid bilayers. Changes to the physicochemical properties of lipid bilayers induced by incorporation of cholesterol will undoubtedly influence the formation of GA ion channels. Relatively little is known/understood about the assemblage of ion channels in spite of their important roles in both maintaining and disrupting cellular integrity. Bilayers composed of lipids with a range of T_M values (-2 to 55 °C) containing cholesterol exist as an ensemble of phases, and serve to sample the landscape of membrane environments in which ion-channels may exist. Understanding, from a lipocentric point of view, how perturbations to the physicochemical interactions of peptide-lipid assemblies affect the conformer preferences of the channel-forming dimerized peptide gramicidin A, ultimately provides further insight into the mechanics and dynamics of other, more complex ion-channel systems. Here, we use ESI-IM-MS to investigate the effects of changes in the physicochemical properties of lipid bilayers, including (i) incorporation of cholesterol, (ii) phase transition temperature, and (iii) incubation time,

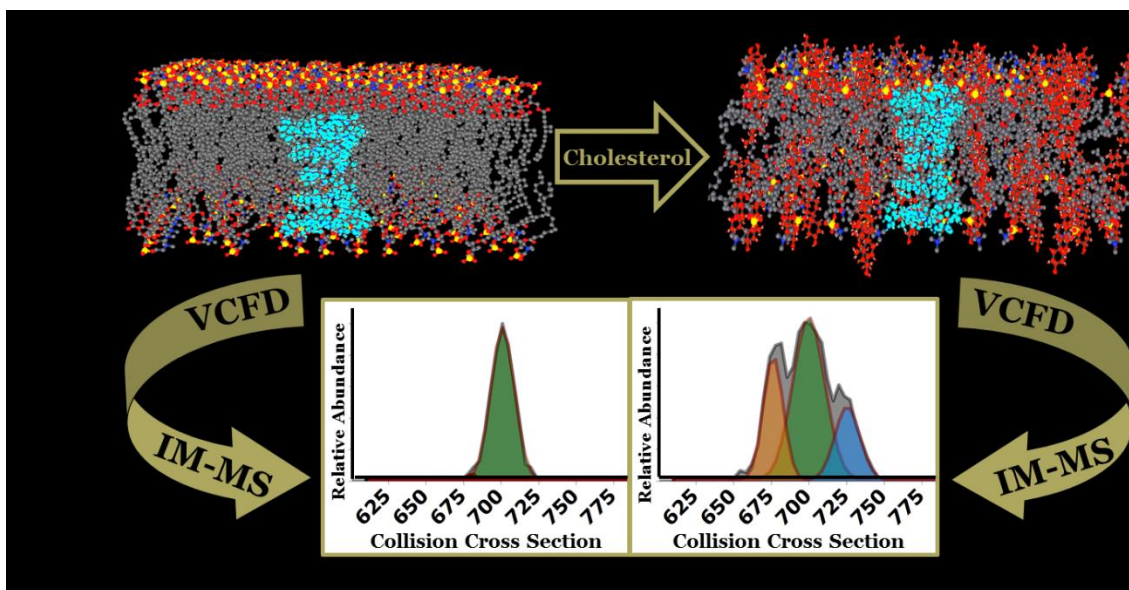


FIGURE 11. Experimental schematic for ESI-IM-MS analysis of gramicidin A (GA) loaded bilayers. VCFD preparation is employed to analyze the effect of altering the physicochemical interactions in the bilayer on the conformational preferences of GA dimers. Depicted are bilayers without cholesterol (left) and with cholesterol (right). Perturbing the physicochemical interactions in the bilayer yields significantly different conformer preferences.

on the conformer preferences of gramicidin A dimers inserted into lipid bilayers (Figure 11). Deviations in GA conformer preferences as a result of modified physicochemical interactions in the bilayer reveal the influence these factors exhibit on the preferred ensemble of ion-channel structures.

Materials and Methods

Gramicidin A amino acid sequence: HCO-L-Val-Gly-L-Ala-D-Leu-L-Ala-D-Val-L-Val-D-Val-L-Trp-D-Leu-L-Trp-D-Leu-L-Trp-D-Leu-L-Trp-NHCH₂CH₂OH

Materials

Gramicidin A (Sigma-Aldrich St. Louis, MO, USA; $\geq 90\%$ purity) was used as received and dissolved in HPLC grade ethanol (Sigma Aldrich St. Louis, MO, USA) at a concentration of 1 mg/mL without further purification. Lipids were received as 10 mg/mL solutions in chloroform (Avanti Polar Lipids, Alabaster, AL) and portioned out into 500 μ L aliquots containing 5 mg of lipid. HPLC grade isobutanol (Alfa Aesar Ward Hill, MA, USA) was used as received.

Vesicle Capture-Freeze Drying Method (VCFD)

Preparation of gramicidin-loaded vesicles was performed according to the VCFD (Vesicle Capture Freeze Drying) method described previously.⁹⁶ Briefly, samples of lipid dissolved in chloroform, and gramicidin A dissolved in ethanol, were combined, dried under nitrogen gas, and subsequently desiccated under vacuum to remove residual solvent. Samples were rehydrated to 1.0 mg/mL lipid in 18 M Ω distilled water, sonicated

30 min and subjected to ten freeze-thaw cycles. Samples were extruded through polycarbonate filters to yield uniform diameter lipid vesicles. Vesicle/GA solutions were allowed to equilibrate at 4 °C overnight prior to freeze drying using liquid nitrogen and a vacuum desiccator. Prior to ESI, lyophilized samples were dissolved in isobutanol for analysis. All electrospray experiments were performed at room temperature. The incubation temperature of each sample differs according to the T_M of each lipid. In the case of lipids with very low T_M such as DLPC, POPC, and DEPC the bilayers were prepared at room temperature, *viz.* above their T_M . Bilayers with higher T_M , such as DPPC and DSPC, were prepared above their T_M . DPPC bilayers were prepared at 55 °C and DSPC bilayers were prepared at 60 °C.

Electrospray – Ion Mobility – Mass Spectrometry (ESI-IM-MS)

ESI-MS and ESI-IM-MS experiments were carried out on a Waters Synapt G2 HDMS (Waters Corp., Milford, MA, USA) equipped with a nano-ESI source operating at ~100 °C. Spectra were acquired in positive ion mode using a 1.5 – 2 KV voltage applied to the capillary tips. ESI tips were manufactured in-house by a gravity-pulled method using fused silica capillary line. Parameters for the traveling wave ion mobility cell were set at 32 V wave height and 400 m/s wave velocity.

All analyses were performed using MassLynx v4.1 software. All reported collision cross section (CCS) values were obtained using a calibration plot from data acquired with instrument conditions identical to those used to analyze GA samples. CCS values for peptide ions, *i.e.*, $[M + 2H]^{2+}$ ions produced by tryptic digestion of myoglobin and cytochrome C, obtained from the Clemmer database were used as calibrants.⁵⁸⁻⁵⁹

CCS calibration was performed as previously described by Ruotolo.⁶⁰ Although there are discrepancies in CCS values obtained using helium versus nitrogen collision gas, reasonable agreement was observed between calibrated CCS and theoretical CCS values reported previously by Chen *et al.* Chen showed that ion mobility peak profiles obtained on the Synapt G2 are sensitive to instrument tuning; however, the experiments described here were all performed using instrument tuning parameters that minimize ion heating.¹⁰¹

High resolution GA spectra were acquired on a Bruker Impact Q-TOF fitted with a Trapped Ion Mobility Spectrometry (TIMS) mobility device. Calibration was performed using ESI Tune Mix (Agilent Tech., Santa Clara, CA, USA). Owing to the location of the TIMS device in the inlet region of the mass spectrometer the gas composition is a mixture of nitrogen and ambient air yielding CCS values that are *ca.* 5% larger than those obtained on Synapt instruments.

All peak-fitting analysis was performed using Origin (OriginLab, Northampton, MA) in order to fit Gaussian peaks to the raw data for each arrival time distribution obtained. The number of peaks fit (*n*) was chosen based on the best representation of the raw data.

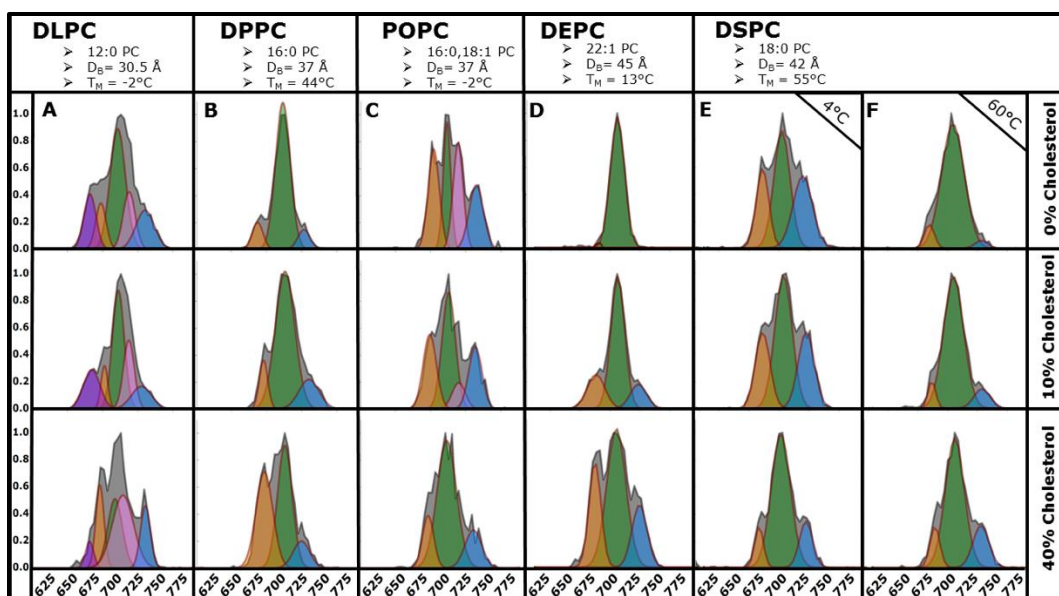


FIGURE 12. CCS profiles for $[2GA + 2Na]^{2+}$ ions electrosprayed from 100 nm DLPC (A), DPPC (B), POPC (C), DEPC (D), and DSPC (E-F) vesicles containing 0-40 mol% cholesterol (vertical, shown at right) plotted as relative abundance vs. CCS (\AA^2). Acyl chain designations, lipid bilayer thickness (D_B), and gel-to-liquid phase transition temperatures (T_M) are provided for each lipid. Vesicle samples were incubated above their T_M , and DSPC was incubated at 4 °C (E) and 60 °C (F). Conformers have been labeled according to the following scheme: Purple – Nascent conformer (660 \AA^2), Orange – PDH (675 \AA^2), Green, Magenta – ADH (700 \AA^2), Blue – SSHH (725 \AA^2).

Results

Effect of Cholesterol on Native GA Conformer Preferences

CCS profiles for GA $[2\text{GA} + 2\text{Na}]^{2+}$ ions from 100 nm vesicles containing 0-40% cholesterol formed from DLPC (12:0 PC), DPPC (16:0 PC), POPC (16:0, 18:1 PC), DEPC (22:1 PC) and DSPC (18:0 PC) prepared using the VCFD methodology are displayed in Figure 12. The conformers shown in Figure 12 have been labeled according to the following color scheme: purple – nascent conformer (660 \AA^2), orange – PDH (675 \AA^2), green, magenta – ADH (700 \AA^2), and blue – SSHH (725 \AA^2). Conformer preferences for samples associated with bilayers devoid of cholesterol, *i.e.* row one of Figure 12, have been discussed in prior work.⁹⁶ Briefly, changes in acyl chain length and extent of acyl chain unsaturation of the vesicle-forming lipids used in these studies were shown to directly alter the conformer preferences of $[2 \text{GA} + 2 \text{Na}]^{2+}$ dimer ions. GA was observed to adopt ADH conformations as the most abundant conformer in each sample. The abundances of PDH and SSHH varied depending on the lipid acyl chain length. The appearance of a nascent (fourth) GA conformer $\sim 660 \text{ \AA}^2$ was also observed from DLPC vesicles (Figure 12A) shown in purple. DSPC, a saturated lipid not explored previously, also adopts primarily ADH conformers, and PDH/SSHH abundances were observed to be dependent on the temperature of incubation as shown in Figure 12, E-F. PDH and SSHH dimers were observed in the highest abundance from samples of POPC as well as DSPC samples incubated at 4 °C.

An increase in cholesterol content of 10 mol% in the bilayer (Figure 12, row 2), resulted in an increased abundance of PDH dimers from DLPC, DPPC, DEPC and DSPC

(60°C) samples (Figure 12 - A, B, D, F, respectively). Abundances of PDH and SSHH dimers from POPC bilayers were observed to decrease slightly upon cholesterol incorporation. For samples of DSPC incubated at 4 °C, the abundances of PDH and SSHH dimers were observed to slightly decrease. Interestingly, the nascent conformer observed from DLPC bilayers decreased in abundance with a subsequent increase in PDH abundance.

The third row in Figure 12 displays the conformer preferences for GA from bilayers containing 40 mol% cholesterol. For all lipids except POPC and DSPC (4 °C) a dramatic increase in PDH and SSHH abundance was observed. Consistent with the trends observed in rows 1 and 2, when the bilayer contained 40% cholesterol the abundance of the nascent conformer from DLPC (Figure 12A) decreased by ~20% whereas PDH abundance increased to ~80%. DPPC and DSPC (60 °C) displayed increases in PDH abundance of ~60% and 50%, respectively. The most significant change in GA conformer preferences was observed from DEPC bilayers which, in the absence of cholesterol, displayed a nearly all-ADH arrangement, but converted to a nearly equal distribution of the three conformers upon increasing the cholesterol content to 40%. DSPC incubated at 4 °C displayed a significant decrease in PDH and SSHH abundance when the cholesterol content was raised to 40% (Figure 12E, row 3). The conformer preferences of GA from DSPC vesicles are similar whether they are obtained from 40% cholesterol bilayers incubated at 4 °C (Figure 12F, row 1) or with 0% cholesterol incubated at 60 °C, *viz.* the ADH conformer is the dominant conformer.

Insight into the conformational heterogeneity of GA dimer populations can be inferred from the peak widths (FWHM) in mobility space obtained from IM-MS measurements where broader peaks indicate a higher degree of heterogeneity. The number of peaks fit (n) was chosen based on the best representation of the raw data for each panel in Figure 12. Peak fitting performed on experimental data where $n = 3$ resulted in poor fits for lipids DLPC and POPC. DLPC was best fit with $n=5$, and Figure 12A shows that as cholesterol content increased, the peak widths for the nascent conformer (purple) narrow as the abundance of the peak decreases. Narrowing is observed for the left-most ADH peak (green) while the second ADH peak fit (magenta) broadens as it increases in abundance corresponding to an increase in the cholesterol content. Additionally, the width of the PDH peak (orange) broadens as cholesterol content increases. PDH peak widths remained unaffected by cholesterol incorporation for other lipids examined in this study. Similarly, POPC was best fit with $n = 4$ suggesting the presence of two conformers under the broad ADH population. DPPC, DEPC, and DSPC were best fit with $n = 3$. The peak deconvolutions presented in Figure 12 represent a mixture of $n = 3$ or 4, except in the case of DLPC, where a nascent peak was observed. Note that $n=4$ peak fits display two ADH peaks which have been colored green and magenta to denote the lower and higher CCS peaks. When $n=3$, only one ADH peak exists and thus has been fit with a green fill only. Figures displaying only $n = 3$ or $n = 4$ peak fits are included in the appendix (Figure A3 and A4) for comparison.

The most intriguing observation arises from examining ADH peak widths for DEPC and DSPC (Figure 12, D-F). ADH peak widths (FWHM) increased from 18.43 Å² with no cholesterol present to 25.04 Å² for DEPC bilayers containing 40% cholesterol indicating an overall increase in the heterogeneity of the ADH population. This phenomenon is observed to be temperature-dependent for DSPC bilayers. ADH peak widths from DSPC bilayers (incubated at 4°C) containing 0% cholesterol were observed to increase from 20.86 Å² to 24.91 Å² with 40% cholesterol present. For DSPC bilayers containing 0% cholesterol (incubated at 60 °C) ADH peak widths were observed to decrease from 29.63 Å² to 24.84 Å² with 40% cholesterol present.

Elucidation of the Structure and Number of ADH Populations Through CCS Profile Peak Fitting and High-resolution TIMS Data

Figure 13 displays CCS profiles for [2 GA + 2 Na]²⁺ ions electrosprayed from 100 nm POPC vesicles. Panels A and B display identical raw data obtained from samples prepared by VCFD methodology on a Synapt G2 HDMS that were fit with three and four peaks, respectively. The same sample was analyzed on a prototype high-resolution IMS instrument (ESI-TIMS-QTOF) (R> 100) with results shown in Figure 13C. Owing to differences in the composition of the drift gas environment, the CCS values obtained are inherently different between these two instruments. Regardless of CCS, the high resolution data revealed two peaks that fall within the range of the ADH region (740-760 Å²) suggesting that ADH populations are composed of two distinct conformers. This is not surprising, as previous investigations on GA dimers using hydrogen deuterium exchange (HDX) revealed two ADH populations with different rates of deuterium

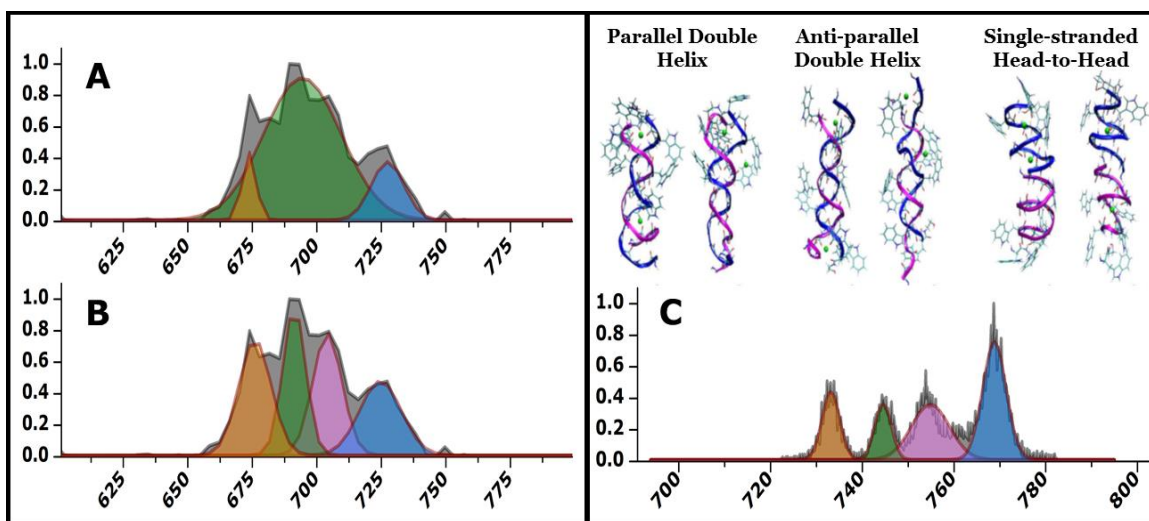


FIGURE 13. CCS profiles for $[2GA + 2Na]^{2+}$ ions electrosprayed from 100 nm POPC vesicles plotted as relative abundance vs. CCS (\AA^2). Panels A and B display identical data obtained on a Synapt G2 ($R \sim 25$) fit using $n = 3$ peak fits (Panel A) and $n = 4$ peak fits (Panel B). Panel C displays high-resolution data obtained on a prototype Bruker TIMS instrument with $R > 100$. Note the magenta nascent peak revealed under the ADH distribution using $n = 4$ peak-fits in Panel B and the high-resolution TIMS instrument. Molecular dynamics (MD) simulations were performed previously to generate candidate structures for each population, and the two most populated structures for each conformer are shown at top right.

exchange.⁶⁴ Additionally, the two most populated clusters produced from MD simulations for each conformer are shown in the top right panel.

Effects of Incubation at Elevated Temperature on Conformer Preferences of Native GA in DSPC Bilayers

Figure 12 demonstrates that GA from DSPC bilayers experiences a significant change in the conformer preferences upon increasing the incubation temperature from 4 to 60 °C (Figure 12, E-F). The effects of incubation time at elevated temperature were examined by incubating DSPC vesicles at 60 °C for periods of 24, 48, and 72 h. Figure 14 displays CCS profiles for $[2\text{GA} + 2\text{Na}]^{2+}$ ions from 100 nm DSPC vesicles containing 0-40% cholesterol incubated at 60 °C for 24 (Fig. 14A), 48 (Fig. 14B), and 72 (Fig. 14C) h, respectively. At all incubation times, SSHH is observed to be most abundant from bilayers containing 40% cholesterol. Figure 14 (A-C) demonstrates that as cholesterol content increases, PDH and SSHH increase in abundance after 24 h of incubation. The magnitude of this increase is greater at longer incubation times, hence, the most significant effect is observed from 72 h of incubation for bilayers containing 40% cholesterol (Fig. 14C).

Discussion

The conformer preferences, multimeric state, and biological functionality of membrane-bound peptides/proteins are sensitive to changes in physicochemical interactions in the bilayer.^{93, 102-103} The physicochemical interactions that dictate bilayer properties such as fluidity *i.e.* lateral mobility of the ensemble of lipids that self-assemble

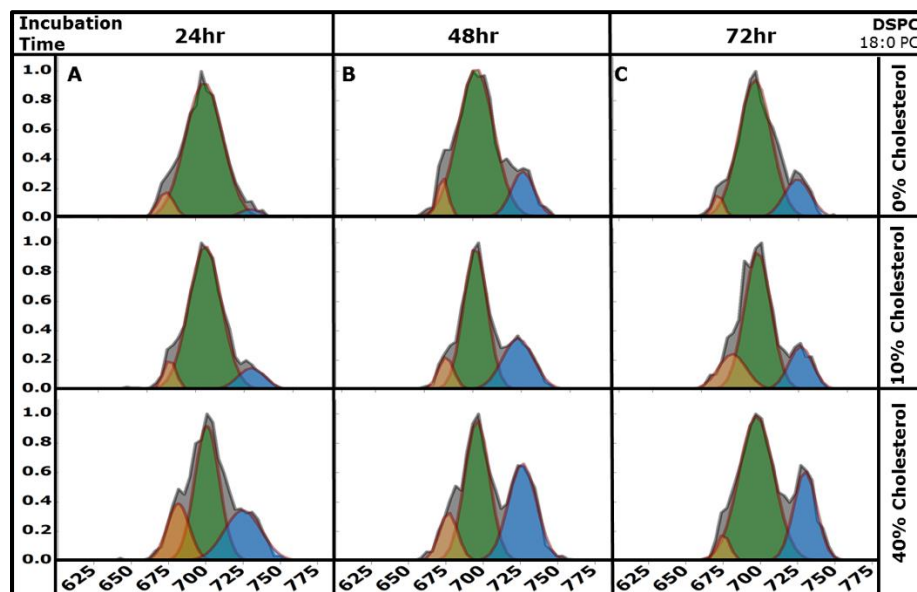


FIGURE 14. Collision Cross Section profiles for $[2GA + 2Na]^{2+}$ ions electrospayed from 100 nm DSPC vesicles containing 0, 10 or 40% cholesterol are plotted as relative abundance vs. CCS (\AA^2). Samples were incubated at 60 °C for 24, 48, and 72 h (Figure 14A, 14B, and 14C, respectively). At all incubation times, SSHH (shown in blue) abundance increases when 40% cholesterol is present.

to form bilayer membranes, can be perturbed through incorporation of small molecules such as cholesterol, or through changes in lipid phase correlating to temperature effects.¹⁰⁰ Herein, the conformer preferences of GA dimers captured from lipid bilayers provide insight into how perturbations of physicochemical interactions influence the ensemble of conformers observed using ESI-IM-MS.

Figure 12 displays CCS profiles for $[2\text{GA} + 2\text{Na}]^{2+}$ ions from vesicles composed of lipids (see figure caption) incorporating 0-40 mol% cholesterol. GA dimer conformer preferences are altered, in a lipid-dependent manner, upon incorporation of cholesterol into the bilayer observed as perturbations in PDH/SSHH abundance and IMS peak widths for ADH conformers. There exists a phenomenon known as the “dual-effect” nature of cholesterol which suggests that the influence of cholesterol on the physicochemical properties of lipid bilayers is dependent upon the temperature of the system in relation to the T_M of a given bilayer. Bilayers formed from lipids with low T_M ($-2\text{ }^\circ\text{C}$), such as DLPC and POPC (Fig. 12A and 12C, respectively) possess relatively disordered lipid acyl chains at room temperature. Introduction of rigid cholesterol into “fluid” bilayers yields an ordering effect on lipid acyl chains, and decreases their lateral mobility. Conversely, disordering effects on acyl chains occur at room temperature if cholesterol is incorporated into bilayers with higher T_M such DPPC, DEPC and DSPC (Fig. 12B, 12D, 12F, respectively). Regardless of temperature, the addition of cholesterol is reported to increase the thickness of the hydrocarbon-rich bilayer interior.

Cholesterol has a direct influence on GA conformer preferences as demonstrated in Figure 12A (DLPC). DLPC bilayers devoid of cholesterol are thin and exhibit moderate

lateral acyl chain mobility at room temperature owing to the low T_M . The appearance of a nascent conformer described previously, shown as the purple peak at 660 \AA^2 , is only observed from DLPC vesicles. We hypothesize that this nascent conformer arises owing to a mechanical compression exerted on the complex only under conditions that exist within very thin bilayers. Upon increasing cholesterol content to 10% or 40% (Fig. 12A, rows 2-3), a decrease in abundance of the nascent conformer was observed. This result is not unexpected; it has long been known that hydrophobic coupling between membrane proteins and acyl chains can yield changes in protein conformation.¹⁰⁴⁻¹⁰⁶ The addition of cholesterol thickens the bilayer, increases lateral lipid mobility, and relaxes positive hydrophobic mismatch and mechanical compression.¹⁰⁷ In fact, Andersen and coworkers have reported that SSHH GA conformers are intimately related to deformations in the bilayer thickness, both contraction and expansion, that influence channel conductance through coupling of hydrophobic thicknesses between GA and acyl chains.¹⁰⁸⁻¹⁰⁹ Accordingly, an increase in bilayer thickness in combination with a decrease in the lateral mobility of acyl chains may explain why SSHH dimers were observed to be more abundant at 10% or greater cholesterol content from DLPC bilayers. Extended acyl chains would permit increased movement and thus would be more likely to adapt to accommodate the relatively wide and bulky SSHH dimer. Further, broadening of ADH IMS peak widths as a function of cholesterol content indicates an increase in the heterogeneity of these populations *viz.* a broader ensemble of populated conformational states.

Vesicles were formed from DEPC (Figure 12D), which yield thicker bilayers than DLPC, in order to study how the effects of cholesterol are related to bilayer thickness. GA complexes associated with DEPC bilayers likely experience negative hydrophobic mismatch, *i.e.* “dimpling of the bilayer”, and have been reported to undergo structural changes.⁷⁴ It was thus hypothesized that thick DEPC bilayers would exert a stretching force on GA dimers. It is not surprising that ADH dimers, hypothesized to anchor themselves on either side of the bilayer via Trp residues positioned at the interface of the solvent/bilayer regions, are the only conformers observed from DEPC vesicles.^{9, 110} Rows 2-3 of Figure 12D support the hypothesis that swelling of the bilayer as a result of cholesterol incorporation may result in the disassociation/rearrangement of these anchored ADH dimers followed by subsequent association/rearrangement of PDH/SSHH. Increases in PDH and SSHH abundance upon increasing amounts of cholesterol in the bilayer (Figure 12A and 12D, rows 2 and 3) were observed from both DLPC and DEPC. We hypothesize this trend arises owing to two opposing mechanisms, that is: i) thickening the bilayer through cholesterol incorporation promotes interconversion from either nascent (DLPC) or ADH conformers to PDH / SSHH dimers, or ii) cholesterol aids in the retention of PDH/SSHH dimer structure.

We hypothesize that changes in conformation that result from the “slipping” apart of GA dimers could be observed using IMS. In fact, the sensitivity of the fitted peak widths for the ADH IMS distributions to cholesterol content discussed above suggests that there exists more than one family of ADH conformers. This hypothesis aligns directly with evidence reported by Durkin and Andersen that SSHH GA dimers can “slip” apart via

breakage of two H-bonds between GA monomers, resulting in an increase in GA monomer bond distance of 0.16nm.^{108, 111} GA has been previously shown to adopt three conformer populations, and GA CCS profiles were originally fit using three total peaks; however in some cases an improved fit was obtained by increasing the number of peaks fit from three (Figure 13A) to four (Figure 13B). Two distinct conformers exist under the broad ADH population observed $\sim 700 \text{ \AA}^2$ at low resolution (Figure 13A, shown in green). This result is not unexpected, as prior MD simulations from our group on GA dimers revealed that ADH exists predominantly as two populations; a smaller CCS complex represents the preferred gas-phase ADH dimer while a larger CCS structure represents partial disassociation (Figure 13, inset). In some cases, ADH peak widths were observed to be insensitive to cholesterol incorporation (POPC, Figure 12C). High-resolution ion mobility data revealed that for GA from POPC, two distinct ADH conformers (Figure 13C) were observed in relatively equal abundance between $730\text{-}770 \text{ \AA}^2$ (shown in green and magenta). We hypothesize that narrowing of the ADH peak widths observed from bilayers formed from DSPC incubated above T_M (Figure 12F) as a function of cholesterol content suggests that depletion of one of these two sub-populations occurs; however, bilayers formed from POPC appear to be particularly resistant to such changes. We have demonstrated the sensitivity of ADH peak widths from DLPC, DPPC, DEPC, and DSPC (Figure 12, A-F) to both acyl chain length and cholesterol content, thus it is reasonable to assume mechanically-stretched complexes will yield a preference for the elongated ADH dimer, and *vice versa*. Further studies are underway utilizing high-resolution TIMS to elucidate how the abundances of ADH sub-structures are perturbed by changes in

physicochemical interactions from bilayers that are sensitive to cholesterol incorporation.

The Effect of Temperature and Incubation Time on GA Conformer Preferences from DSPC Bilayers

The lipid bilayer in eukaryotic organisms is a heterogeneous landscape owing to the diverse nature of membrane-active peptides and proteins. The integral role that temperature plays on the phase-behavior of lipid bilayers *viz.* changes in the physicochemical interactions of the acyl chains has been understood for many years.⁷² Native bilayers remain at a relatively constant temperature and organisms rely on the enrichment of a number of lipids with specific physical properties *i.e.*, alkyl chain length and extent of unsaturation, to govern peptide- or protein-lipid physicochemical interactions. The complexity of these natural bilayers makes characterization of specific interactions between lipids and peptide or protein difficult. In order to further understand how changes in bilayer phase behavior affect the conformer preferences of GA complexes, the effects of varying the temperature of a well-understood mono-component DSPC lipid bilayer were examined.

High T_M lipids provide a unique system wherein lipid bilayer phase behavior can be manipulated through temperature control of the bilayer. At low temperature, DSPC bilayers remain in the S_O (gel-like / solid ordered) phase and thus the lateral mobility of the lipids comprising the bilayer is restricted. At temperatures above the T_M of DSPC (55 °C), the lipid acyl chains increase in lateral mobility yielding an L_D (liquid-disordered) phase.¹¹² An additional L_O (liquid ordered) phase exists when cholesterol is present in sufficient quantity below the T_M of a given lipid wherein lipid acyl chains are ordered as

in the S_0 phase yet retain increased lateral mobility. Phase behavior can be tuned owing to the high T_M of DSPC to permit observations on how GA conformer preferences are affected in S_0 vs. L_D phases. The appearance of an L_O phase provides insight into the differences in GA conformer preferences observed when perturbing a system that originally exists predominantly in the S_0 vs. L_D phases.

At 4 °C, the DSPC bilayer exists in the S_0 phase where lipid acyl chain lateral mobility is limited and an abundance of all three conformers – PDH, ADH, SSHH – were observed (Figure 12E), shown in orange, green, and blue, respectively. Introducing cholesterol (Figure 12E, rows 2-3), increased acyl chain lateral mobility at low temperature, likely through formation of an L_O phase, yielding a CCS profile that appears similar to DSPC incubated above T_M (Figure 12F). This observation supports the notion that DSPC bilayers containing GA and cholesterol, when incubated above the T_M , may experience decreased lateral mobility owing to the presence of cholesterol. We hypothesized that above T_M , DSPC would behave similar to DEPC wherein ADH dimers appeared to convert to PDH/SSHH as a function of cholesterol content. Nagao and coworkers demonstrated that a negative hydrophobic mismatch occurs between GA in L_O phase DSPC bilayers, and similar trends in PDH/SSHH abundance as demonstrated from DEPC are observed in DSPC.¹¹³ Our observations from DSPC suggest that gel-like bilayers preserve conformer preferences adopted in the S_0 phase, as evidenced by the increased abundances of PDH and SSHH dimers when comparing Figure 12E to 12F. Elevating the incubation temperature above T_M increases acyl chain mobility allowing rearrangement to primarily ADH dimers. DEPC, a longer acyl chain lipid (Figure 12D),

did not adopt similar temperature-related behavior which may be attributed to points of unsaturation in its acyl chain. Unsaturation of the acyl chains introduces disorder through the addition of kinks in the chain typically yielding bilayers with much lower T_M than their saturated-chain analogs. Upon increasing cholesterol content, above T_M , lateral mobility of the lipids are reduced such that GA conformer preferences in DSPC appeared more similar to those observed from S_o -phase bilayers despite the bilayer existing as a mixture of L_o/L_D phases. Under conditions of increased incubation temperature/time the bilayer remains relatively fluid and thus ADH, the preferred conformer, is not disrupted by perturbations of the bilayer phase.

Length of Incubation on Conformer Preferences of GA in DSPC Bilayers

Figure 14 demonstrates that SSHH abundance at 40% cholesterol increases as a function of incubation time, indicating that over longer timescales formation of the head-to-head dimer complex becomes more favorable. This result is not entirely unexpected, as Killian and coworkers reported that incubation of a GA sample at ~ 70 °C promotes rearrangement into SSHH conformers.²⁶ ADH peak widths for 40% cholesterol significantly broadened after 72 h incubation when compared to 24-48 h of incubation. The broadening observed for ADH suggests that the bilayer environment is changing, after 72 h, as denoted by changes in the abundances of ADH conformers. This argument is further supported by the disappearance of PDH dimers. The abundance of SSHH after 48 h did not change, suggesting that at higher temperature, longer timescales, and with more cholesterol present, SSHH dimers are more stable than PDH or ADH conformers. For some time it has been reported that cholesterol can aggregate in bilayers to form “rafts”

or regions of cholesterol enrichment resembling patches on the bilayer surface.¹¹⁴⁻¹¹⁶ The effects observed here may result from a redistribution of cholesterol in the bilayer. SSHH formation appears to be promoted by the organizing effect on acyl chains that arise from the presence of cholesterol above T_M along with decreased lipid lateral mobility. The association of monomers embedded in either the exterior or interior leaflet has been proposed as the primary mechanism for SSHH formation.¹⁰⁸ We hypothesize that GA monomers from DSPC bilayers, under extended incubation times in the presence of cholesterol, experience enhanced formation of head-to-head dimers owing to the decrease in lipid lateral mobility promoting increased GA-GA interactions. Figure 14A demonstrates that 24 h incubation is sufficient, in the presence of 10-40 % cholesterol, to increase SSHH abundance. This evidence suggests that decreases in the lateral mobility of lipids as a result of cholesterol incorporation promotes the association of GA monomers yielding an increase in SSHH abundance. While further studies are underway to probe this phenomenon, it is evident that the conformer preferences observed for GA dimers are a result of incubation time as well as competing physicochemical interactions between cholesterol and lipid acyl chains.

Conclusion

Understanding how factors that govern the physicochemical properties of lipid bilayers affect the conformer preferences of biomolecules is a unique challenge emerging at the interface of analytical chemistry, biology, and biophysics. Herein, we successfully demonstrate the use of VCFD coupled to ESI-IM-MS to provide insight into the effects of cholesterol incorporation, incubation temperature, and incubation time on GA dimer

conformer preferences associated with lipid vesicle bilayers. We have previously shown that the conformer preferences of GA dimers are dependent on the composition of the lipid bilayer with which they associate. Here, we have shown that the incorporation of cholesterol into the bilayer yields an increased abundance of SSHH dimers and increases peak widths for ADH conformers. For bilayers formed from DSPC (18:0 PC), which possess a high T_M (55 °C), we observed that GA conformer preferences varied significantly upon incubation above or below the lipid's T_M . Incubation above T_M yielded a lower abundance of PDH and SSHH dimers whereas incubation below T_M yielded an ensemble of all three GA dimer conformers. Cholesterol was observed to alter the conformer preferences of GA dimers from DSPC in a temperature dependent manner. Above T_M , the addition of cholesterol yielded narrowed ADH distributions and increased PDH and SSHH abundance. Conversely, below T_M the addition of cholesterol yielded decreased PDH and SSHH abundance with broader ADH populations. These results suggest that cholesterol directly affects the lateral mobility *i.e.* fluidity of the lipid bilayer in a temperature dependent manner. Increasing incubation time of a sample of DSPC, above T_M , yielded an increase in SSHH abundance as well as a broadening of the ADH dimer peak corresponding to an increase in cholesterol content in the bilayer. This study elucidates the role that temperature, cholesterol incorporation, and incubation time play on the conformer preferences of the model ion-channel gramicidin A using IM-MS. More importantly, VCFD coupled to IM-MS provides a means by which comparisons can be made to relate changes in various physicochemical interactions with the far-reaching effects these changes have on peptide/protein structural preferences.

CHAPTER V

RAPID CAPILLARY MIXING EXPERIMENTS FOR THE ANALYSIS OF
HYDROPHOBIC MEMBRANE COMPLEXES DIRECTLY FROM AQUEOUS LIPID
BILAYER SOLUTIONS

Introduction

The ability to investigate the conformational preferences of peptides and proteins directly from their native state stands at the forefront of interdisciplinary efforts from both biological and chemical fields. Recent innovations in mass spectrometry have permitted the characterization of not only the mass to charge ratio (m/z) of biomolecules but also the size and shape of analytes using ion mobility mass spectrometry (IM-MS). Recent efforts by the Bush, Robinson, and Ruotolo groups have focused on the characterization of biomolecules from a native (or native-like) state wherein the peptides or proteins are electrosprayed using solution conditions that represent physiological conditions with respect to ionic strength and pH.¹¹⁷⁻¹¹⁹ Significant challenges exist, however, for membrane associated peptides and proteins that reside in the hydrophobic internal region of lipid bilayers. Recent advances in high resolution mass spectrometry and IM-MS have enabled previously unprecedented analysis of membrane protein structure.^{65, 120-121}

*Reprinted with permission from “Rapid Capillary Mixing Experiments for the Analysis of Hydrophobic Membrane Complexes Directly from Aqueous Lipid Bilayers” by Patrick, J.W.; Zervas, B.L.; Gao, J.; Russell, D.H., *Analyst*, 2016, DOI:10.1039/C6AN02290A. Reproduced by permission of The Royal Society of Chemistry.

There exists a need for novel experimental techniques for MS analysis of membrane protein / peptides as these molecules are typically electrosprayed in the presence of lipids or non-ionic detergent molecules, such as n-dodecyl β -D-maltoside (DDM) and tetraethylene glycol monoethyl ether (C8E4), to maintain native protein structure in the gas phase.¹²²⁻¹²³ Nanodiscs have been employed by the Gross and Klassen groups to capture membrane proteins in planar disc-like lipid bilayers, however, this technique yields convoluted spectra congested by peaks from the nanodisc scaffold protein.¹²⁴⁻¹²⁵ Recently, it has been shown that using Vesicle Capture Freeze Drying (VCFD) methodology permits the analysis of the conformer preferences of a hydrophobic membrane peptide complex, gramicidin A (GA), from lipid vesicle bilayers.¹²⁶⁻¹²⁷ While effective, this process requires a lengthy freeze-drying protocol that extends the preparation time of samples prior to MS analysis. Sharon and Konermann have demonstrated mixing tee - electrospray ionization (MT-ESI) as a technique for analyzing proteins on shorter kinetic timescales than standard ESI methodologies.¹²⁸⁻¹²⁹ MT-ESI allows for fast mixing between organic solvent (isobutanol) and aqueous solutions of lipid vesicles containing GA, removing the need for lengthy VCFD preparation. The disassociation of lipids during ESI, owing to a loss in the hydrophobic forces driving bilayer formation, results in the ejection of GA dimer complexes into the droplet. MT-ESI provides, for the first time, access to the conformer preferences of GA molecules analyzed directly from aqueous solution using IM-MS. Herein, a novel technique is described wherein rapid mixing of lipid vesicle bilayers containing GA from an aqueous solution

are electrosprayed directly without freeze-drying for the analysis of lipid-associated conformer preferences.

Methods

The mixing tee - ESI (MT-ESI) apparatus was prepared using a mixing tee (IDEX Health & Science Oak Harbor, WA, USA) with 29.0 nL dead volume arranged in a T-shape wherein two identical length capillaries of 75.0 μm diameter were arranged in a head to head fashion terminating in a 5.0 cm capillary of 50 μm diameter to allow transfer of the mixed solution to the fused silica ESI emitter prepared in house. A schematic of the setup is shown in Figure 15. Mixing time for this setup is estimated to be ca. 0.38 s using a 2.0 $\mu\text{L}/\text{min}$ flow rate. In all MT-ESI experiments solution #1 contained aqueous samples of lipid vesicles containing GA at ca. 20 μM ; solution #2 was isobutanol (Sigma-Aldrich St. Louis, MO, USA).

Gramicidin A (Sigma-Aldrich St. Louis, MO, USA) was used as received and dissolved in HPLC grade ethanol (Sigma Aldrich St. Louis, MO, USA) at a concentration of 1.0 mg/mL. Lipids were used as received in 10.0 mg/mL solutions in chloroform (Avanti Polar Lipids, Alabaster, AL). HPLC grade isobutanol was used as received (Sigma-Aldrich St. Louis, MO, USA).

Experiments were performed on a SYNAPT G2 HDMS equipped with an electrospray ion source and MassLynx 4.1 data processor (Waters Corp., Milford, MA, USA). Determination of GA CCS values was performed according to methods previously described by Ruotolo and coworkers.¹³⁰

Results and Discussion

The most prominent barrier prohibiting the MS analyses of membrane peptides and proteins from their membrane environment remains to be their inability to be electrosprayed directly from aqueous solution. Efforts to analyze membrane-bound biomolecules using ESI have previously circumvented this issue through the use of nonionic detergents, nanodiscs, and freeze-drying preparatory methods.¹³¹⁻¹³² While vesicle capture - freeze drying has previously provided access to the conformer preferences of lipid bilayer associated gramicidin A (GA) dimer complexes, this method requires lengthy freeze drying steps that extend preparation time by ca. 8 h. Novel on-line sample introduction to the mass spectrometer using MT-ESI yields ca. 50% reduction in sample preparation time and the ability to analyze GA directly from lipid bilayers suspended in aqueous solution.

Figure 16 depicts the utility of mixing tee - electrospray ionization (MT-ESI) for the analysis of lipid bilayer associated GA from aqueous solution. GA is only sparingly soluble in water (nanomolar equivalents) yielding no appreciable ion abundance during typical ESI as demonstrated in Figure 16A.¹³³ Mass spectra are shown for $[2GA + 2Na]^{2+}$ ions electrosprayed from POPC (B) and DEPC (C) bilayers, respectively, using the MT-ESI setup wherein abundant GA signal is observed around m/z 1904. Figure 17 depicts CCS profiles for $[2GA + 2Na]^{2+}$ ions electrosprayed from (A,C) POPC and (B,D) DEPC bilayers. Data in Figures 17A and 17B were obtained using VCFD preparation, whereas for Figures 17C and 17D data were obtained using an MT-ESI setup. The conformers shown in Figure 17 have been labeled according to the following color scheme: orange,

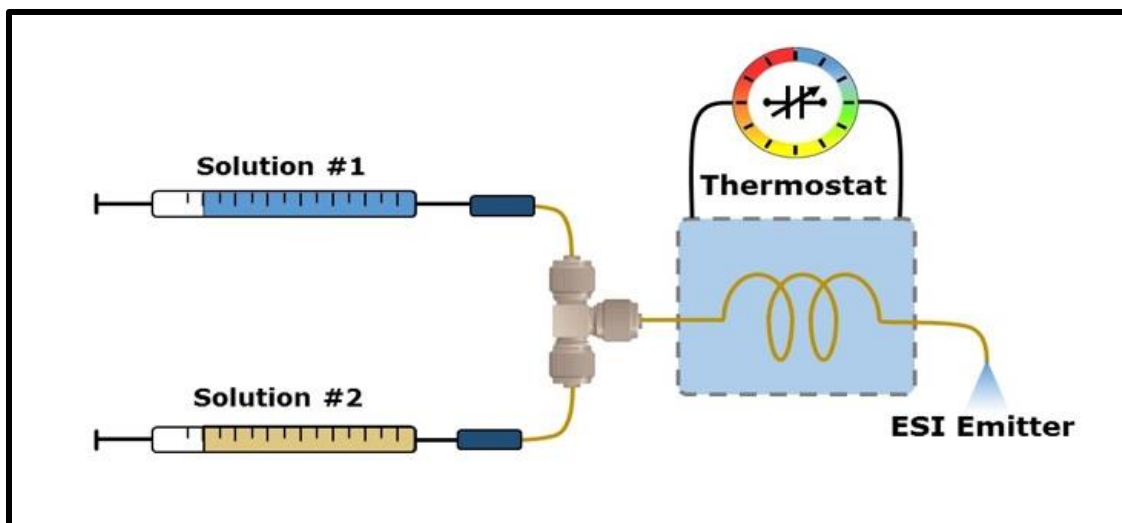


FIGURE 15. ESI coupled to the mixing tee setup reduces sample preparation time by *ca.* 50% compared to VCFD methodology. GA conformer preferences are obtained directly from lipid bilayers suspended in aqueous solution (solution #1) combined with isobutanol (solution #2).

PDH (675 \AA^2); green, antiparallel double helix (ADH) (700 \AA^2); and blue, SSHH (725 \AA^2). The abundance of parallel double helix (PDH) and single-stranded head-to-head (SSHH) dimers, observed around 675 and 725 \AA^2 respectively, electrosprayed using MT-ESI from POPC bilayers is lower than previously reported.¹²⁶⁻¹²⁷ HDX studies on GA from alcoholic solutions have revealed that double-helical GA dimers exhibit fast and slow exchange kinetics wherein PDH dimers exchange at a faster rate than ADH dimers observed around 700 \AA^2 .¹³⁴ This difference in exchange kinetics was attributed to unwinding of the C-terminal regions of the PDH dimer increasing the solvent accessibility of the complex. In addition, Wallace and coworkers have reported that SSHH dimer complexes contain only 6 intermolecular H-bonds responsible for complex association.¹³⁵⁻¹³⁶ In light of these findings, it is not surprising that PDH and SSHH dimers are lower in abundance when exposed to aqueous solutions even under the short timescale of the MT-ESI experiment. Chen and coworkers have demonstrated that ADH dimer complexes both monomerize and undergo deuterium exchange at slower rates than do PDH/SSHH, suggesting these dimers are both less kinetically stable and more solvent accessible than ADH dimers.¹³⁴

DEPC dimers in particular demonstrate very good agreement with prior VCFD results. Previously, it was hypothesized that the dominance of ADH conformers observed from DEPC bilayers with a relatively thick diameter was a result of stretching forces between Trp-rich C-termini that anchor the complex on either side of the bilayer's solvent interface.^{126-127, 137} MT-ESI results in Figure 17D suggest that i) VCFD methodology

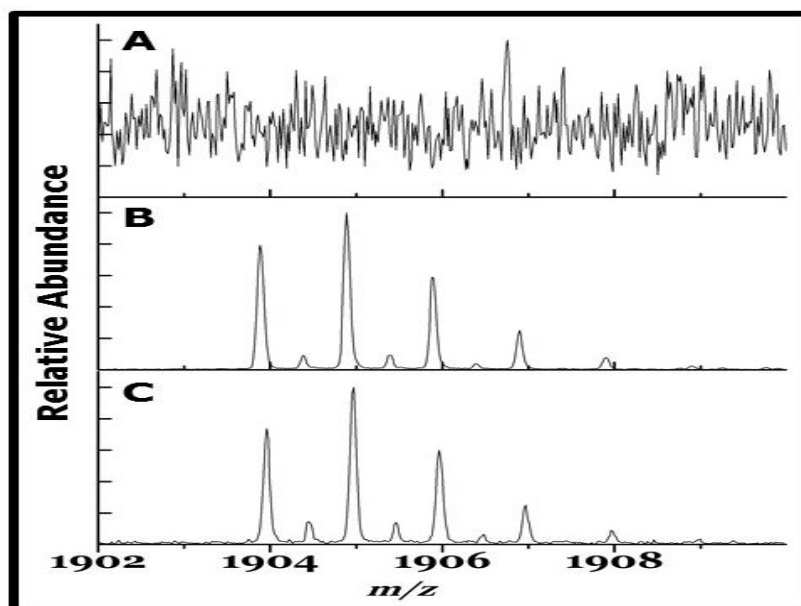


FIGURE 16. Panel A: ESI mass spectrum for $[2 \text{ GA} + 2 \text{ Na}]^{2+}$ ions electrosprayed from an aqueous solution containing GA inserted in 100nm POPC vesicles. Panels B and C: GA dimer ions analyzed from 100nm vesicles of POPC and DEPC, respectively, using MT-ESI. Note the lack of GA signals in Panel A as a result of the extremely low solubility of GA in aqueous solution.

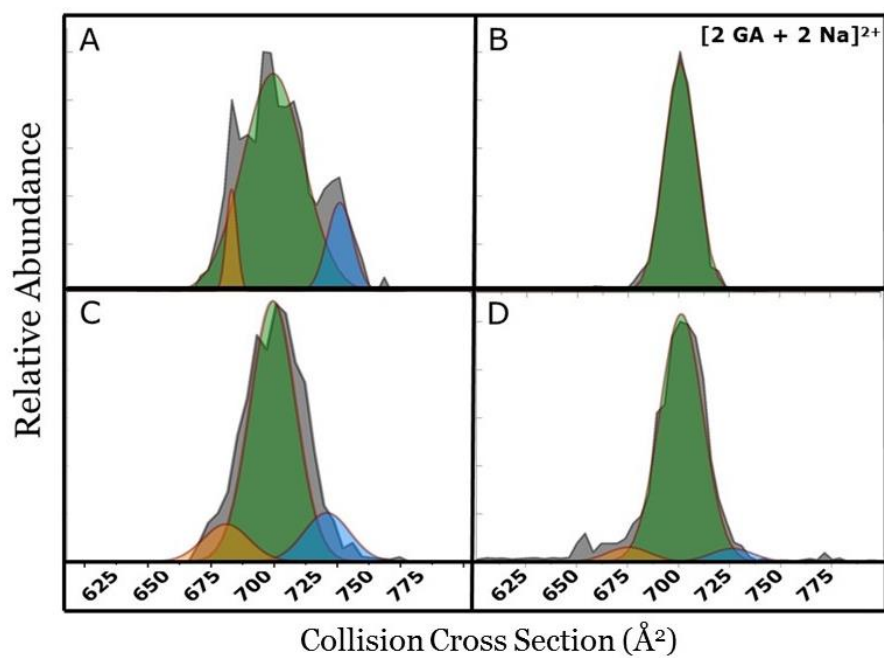


FIGURE 17. Collision Cross Section (CCS) profiles for $[2\text{GA} + 2\text{Na}]^{2+}$ ions electro sprayed from 100nm POPC (A,C) and DEPC (B,D) vesicles. Panels A and B were acquired using Vesicle Capture - Freeze Drying (VCFD) methodology. Profiles in C and D were acquired using MT-ESI of solutions containing aqueous vesicle solutions and isobutanol. Conformers have been labeled according to the following scheme: orange, PDH (675 \AA^2); green, ADH (700 \AA^2); blue, SSHH (725 \AA^2).

samples GA conformer preferences at relatively short kinetic timescales and ii) VCFD methodology does not significantly alter the native conformer preferences that GA adopts in the bilayer. While the aforementioned techniques yield similar information on the conformer preferences adopted by GA from lipid bilayers, the shorter preparation time required for analysis using MT-ESI coupled with the ability to directly sample GA conformer preferences from aqueous solutions of lipid vesicles underscores the utility of this novel technique.

MT-ESI Reveals Conformer Preferences for Novel GA Analogues Containing Hydrophilic Sites

Owing to dramatic increases in the resistance of bacteria to treatment by antibiotic drugs there exists a growing demand for novel antibiotic compounds. Among novel antibiotics, perhaps the most alluring and least understood is the category of antimicrobial peptides (AMPs). Increased understanding of the underlying mechanisms of action (MOA) that facilitate antimicrobial peptide (AMP) /protein activity on bacterial membranes is imperative to our ability to tailor their use as antibiotics. The MOA of AMPs cannot be predicted using primary sequence alone.¹³⁸ In tandem with the growing need to develop novel antibiotics to combat drug-resistant bacteria, it is clear that novel techniques must emerge to provide an increased understanding of the interactions between AMPs and lipid bilayer membranes. Zervas and coworkers have demonstrated the ability to tune the therapeutic properties of GA dimers through the introduction, and functionalization, of lysine residues substituted for leucine residues at positions 10, 12, and 14 of the wild type (WT) GA sequence.¹³⁹⁻¹⁴⁰ Herein, phospholipid vesicles are

utilized to elucidate the effect of introducing hydrophilic sites on the conformer preferences of GA complexes using MT-ESI-IM-MS. Novel MT-ESI sample preparation methodology enhances sample throughput and provides previously unobtainable conformer preferences for GA analogue ions.

Figure 18 displays CCS profiles obtained using MT-ESI for GA analogues incorporating 3 Lys residues (GA3K) as well as a modified analogue containing singular isopropyl modifications to the lysine headgroup (denoted GA3K(ipr)). Panels A and D depict the conformer preferences for sodiated dimer ions of GA3K and GA3K(ipr), respectively, electrosprayed directly from isobutanol. Under these conditions, both GA analogues adopt a compact structure (ca. 635 \AA^2) indicating that in solution, both modified and unmodified lysine residues facilitate the adoption of a compact structure that is not observed for WT GA. Previously, only the conformer preferences of GA from phosphatidylcholine (PC) lipid bilayers have been investigated using VCFD methodology. Lipid vesicles were prepared using 50/50 POPC/POPG lipids in an attempt to simulate the exterior surface conditions of bacterial membranes upon which native GA is known to interact. This preparation yields an enrichment of negatively charged phosphatidylglycerol (PG) headgroup lipids on the exterior the vesicle bilayers. POPC/POPG vesicles were prepared at 100 nm diameter to compare directly with MT-ESI results using WT GA. MT-ESI results shown in Figure 18 reveal that i) binding of GA3K mutants occurs on the timescale of several minutes and ii) GA3K mutants adopt similar ADH (or ADH-like) conformations upon lipid binding. The timescale of lipid

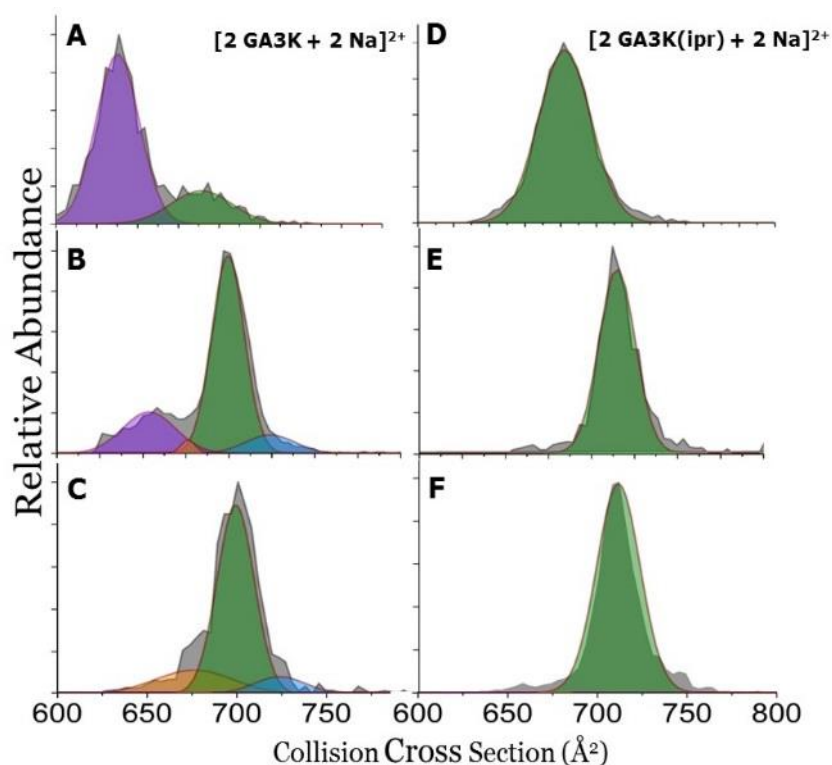


FIGURE 18. Collision Cross Section (CCS) profiles for GA mutant dimer ions. Shown at left are data for $[2\text{GA3K} + 2\text{Na}]^{2+}$ ions electro sprayed from isobutanol (A) and 100nm POPC/POPG (16:0, 18:1 PC/PG) vesicles incubated for either 10.0 min or 24 h (B and C, respectively). Shown at right are CCS profiles for $[2\text{GA3K(ipr)} + 2\text{Na}]^{2+}$ ions electro sprayed from isobutanol (D) and 100nm POPC/POPG (16:0, 18:1 PC/PG) vesicles incubated for either 10.0 min or 24 h (E and F, respectively). Lysine headgroups on GA3K(ipr) have been modified to include single isopropyl (ipr) groups. GA mutants incorporating lysine were observed to adopt ADH conformers for both the modified and unmodified amine headgroup variants. Conformers have been labeled according to the following scheme: purple, compact conformation (635 \AA^2); orange, PDH (675 \AA^2); green, ADH (700 \AA^2); blue, SSHH (725 \AA^2).

binding is unsurprising as electrostatic interactions are likely to promote binding between GA3K mutants carrying positively charged lysine residues and negatively charged PG headgroups residing on the exterior leaflet of the lipid vesicles.¹⁴¹⁻¹⁴² Figure A5 demonstrates that the addition of 10.0 % water to a sample of GA3K electrospayed from isobutanol depletes the abundance of PDH/ADH dimers yielding only the compact conformer $\sim 635 \text{ \AA}^2$. This phenomenon suggests that the conformer preferences observed for the lipid associated samples of GA3K and GA3k(ipr) (Fig. 18B,C,E, F) are owed to association with the lipid bilayer and do not arise from solution phase interactions. The adoption of ADH (or ADH-like) conformations by GA is not unexpected as this behavior has been observed across a wide range of PC lipids. Previous investigations using VCFD methodology have revealed that deformylation of the N-termini of GA monomers yields primarily PDH and SSHH dimers. It is surprising that the introduction of basic sites by incorporating lysine residues on the C-terminal portion of GA promotes adoption of ADH, and not PDH or SSHH dimers. Heterodimers consisting of one deformylated and one formylated monomer of WT GA were previously observed to adopt ADH and SSHH conformations.¹²⁶ This suggests that destabilization of the dimer complex occurs upon disruption of peptide N-termini.

Figure 19 shows representative structures for GA3K dimers with side chains for lysine and tryptophan residues shown in red and black, respectively. We hypothesized that an ADH-like conformer would be most preferred for GA3K owing to the distribution of lysine residues across the entire length of the dimer complex that would minimize sterically/electrostatically unfavorable lys-lys interactions while also promoting

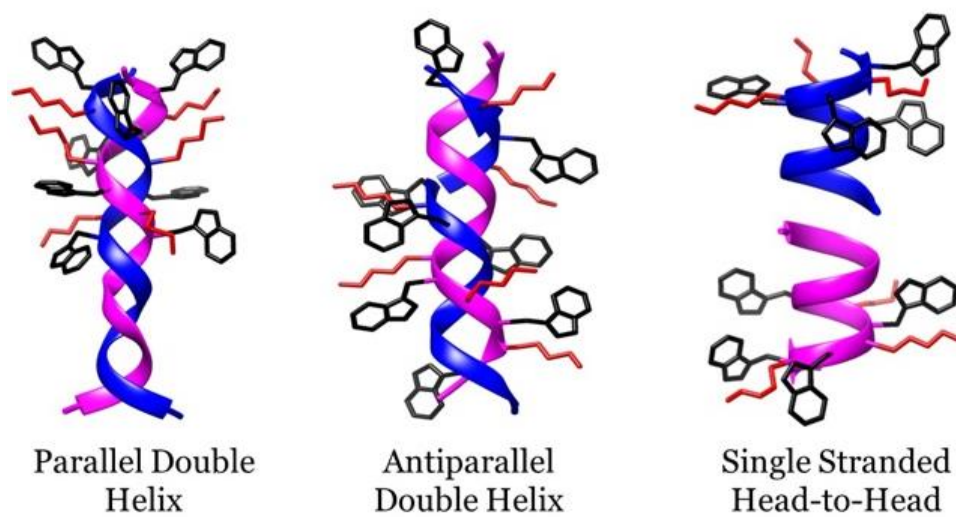


FIGURE 19. Structural depictions of GA3K dimers. Shown in blue / magenta are GA monomers containing Leu to Lys modifications. Sidechains for Lys and Trp residues are shown in red and black, respectively.

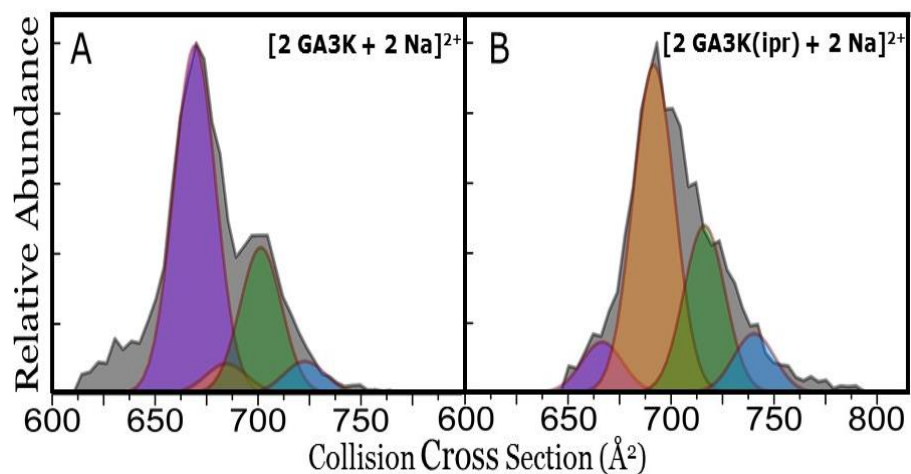


FIGURE 20. Collision Cross Section (CCS) profiles for [2GA3K + 2Na]²⁺ (A) and [2GA3K(ipr) + 2Na]²⁺ (B) ions electrosprayed from 100 nm DLPC/DLPG (12:0 PC/PG) vesicles incubated for 10.0 min. Profiles were acquired using the mixing tee apparatus containing aqueous vesicle solutions and isobutanol. Nascent conformers are observed from DLPC bilayers in both modified (ipr containing) and unmodified GA3K dimers. Conformers have been labeled according to the following scheme: purple, nascent conformation (660 Å²); orange, PDH (675 Å²); green, ADH (700 Å²); blue, SSHH (725 Å²).

stabilizing interactions between Lys and amphiphilic Trp residues. It was previously reported that GA3K did not cause noticeable K⁺ ion leakage from human red blood cells even at 100 μ M.¹⁴⁰ Investigations into the structure of these analogues were not performed, however these results agree with our observations that GA3K adopts predominantly ADH dimers that cannot conduct monovalent cations as efficiently as the SSHH complexes observed from native GA dimers.

The VCFD methodology has been shown to reveal the conformer preferences of WTGA dimer complexes from a range of lipid bilayers prepared using PC lipids with varying acyl chain lengths. DLPC yields thin bilayers owing to its short (12 carbon) acyl chains. A nascent GA conformer was previously reported when GA was electrosprayed from 100 nm DLPC vesicles.¹²⁶⁻¹²⁷ MT-ESI was used to investigate the conformer preferences of GA3K and GA3K(ipr) from DLPC/DLPG vesicles in order to determine how the conformer preferences of these modified analogues are perturbed when associated with thin bilayers. Figure 20 displays the conformer preferences of GA3K (A) and GA3K(ipr) (B). [2GA + 2Na]²⁺ ions electrosprayed from 100 nm DLPC/DLPG vesicles. The most distinct difference in conformer preferences between GA3K and GA3K(ipr) is the adoption of a nascent conformer observed at $\sim 660 \text{ \AA}^2$ from GA3K (Figure 20A). For GA3K(ipr) the population of this nascent conformer and that of the PDH dimer were observed to invert, suggesting that the modified GA3K forms more stable PDH complexes in thinner DLPC bilayers. The appearance of a nascent conformer in DLPC bilayers was previously hypothesized to result from mechanical compression of GA dimers. The results shown in Figure 20 suggest that GA3K(ipr) is more resistant to the formation of this

nascent, compressed conformer. The addition of isopropyl groups to the lysine head groups would be expected to sterically hinder the compaction of GA conformers, and this result is consistent with phenomena observed in Figure 20.

Conclusions

The growing field of antimicrobial peptide and protein therapeutics necessitates the development of novel techniques with which the structure and mechanisms of action can be investigated. Ion mobility - mass spectrometry (IM-MS) is a rapidly developing tool in the arsenal of scientists interested in the characterization of peptide and protein biophysics. The use of mixing tee - electrospray ionization (MT-ESI) has been demonstrated as a novel ESI apparatus to shorten preparation time and facilitate the analysis of Gramicidin A (GA) associated with lipid vesicle bilayers. Herein, the ability to electrospray GA dimers directly from aqueous suspensions of lipid bilayers has been demonstrated for the first time. MT-ESI reduces preparation time for these samples by 50%. Modified GA analogues (GA3K and GA3K(ipr)) containing lysine residues substituted for leucine residues at positions 10, 12, and 14 afford investigations into i) how conformer preferences change upon the introduction of hydrophilic sites into the sequence, and ii) investigations into interactions between a cationic ion channel complex and negatively charged lipid bilayer containing phosphatidylglycerol (PG) head groups.

CHAPTER VI

SUMMARY AND FUTURE OUTLOOK

Summary

The use of electrospray ionization (ESI) for the study of peptides and proteins has developed significantly over the past 30 years owing to technological advancements and increased utilization by research groups in biologically related fields of study. In this dissertation, we used nano-ESI coupled to ion mobility mass spectrometry (IM-MS) to study the self-assembled hydrophobic peptide dimer of Gramicidin A (GA). Owing to the loss of the hydrophobic forces driving the association of peptide / protein dimers during the transfer of an analyte into the gas phase ESI has previously been underutilized as a biophysical tool.

The development of novel preparatory techniques has facilitated the analysis of GA dimers directly from a lipid bilayer environment. The vesicle capture-freeze drying (VCFD) method was developed to provide a novel approach to study gas-phase dimer ion conformer distributions of hydrophobic peptide complexes. GA dimer complexes successfully captured by lipid vesicles suspended in aqueous solution were analyzed using the VCFD method to monitor the conformer preferences of dynamic dimers. A detailed description of this process was provided in Chapter III. Initial studies using this technique revealed that GA dimer conformer preferences are (i) affected by incorporation into lipid bilayer membranes as well as solutions containing lipids, and (ii) solution-phase physico-chemical interactions influenced by lipids could be probed by monitoring the conformer

preferences using IM-MS. Through altering phospholipid properties such as the acyl chain length and the extent of acyl chain unsaturation it was revealed that differences could be observed in the conformer preferences of the dimer ions. The VCFD methodology made possible, for the first time, the direct measure of the gas-phase conformer preferences of lipid bilayer bound GA dimers from an originally aqueous solution using ESI-IM-MS. The results obtained using VCFD methodology coupled to IM-MS demonstrate that the gas-phase conformer distributions sampled by ESI-IM-MS are directly related to the ensemble of conformers observed in the solution phase.

The lipid bilayer is a diverse landscape occupied not only by a variety of lipids that influence the activity of peptides and proteins but by an array of small molecules that modify the physicochemical properties of the lipid bilayer. To this extent, we set out to study the effect that including small molecules, such as cholesterol, would have on the conformer preferences of GA dimers inserted in a lipid bilayer. Chapter IV demonstrated the use of VCFD coupled to ESI-IM-MS to provide insight into the effects of cholesterol incorporation, incubation temperature, and incubation time on GA dimer conformer preferences associated with lipid vesicle bilayers. As demonstrated in Chapter III, the conformer preferences of GA dimers are dependent upon the composition of the lipid bilayer with which they associate. Chapter IV revealed that the incorporation of cholesterol into the bilayer yielded an increased abundance of single stranded head-to-head (SSHH) dimers and increased peak widths for antiparallel double helix (ADH) conformers. For bilayers formed from DSPC (18:0 PC), which possess a high gel to liquid transition temperature (T_M) of 55 °C, it was observed that GA conformer

preferences varied significantly upon incubation above or below the lipid's T_M . Incubation above T_M yielded a lower abundance of parallel double helix (PDH) and SSHH dimers whereas incubation below T_M yielded an ensemble of all three GA dimer conformers. Using the VCFD approach, it was observed that cholesterol alters the conformer preferences of GA dimers from DSPC bilayers in a temperature dependent manner. Above T_M , the addition of cholesterol yielded narrowed ADH distributions and increased PDH and SSHH abundance. The addition of cholesterol below T_M yielded decreased PDH and SSHH abundance with broader ADH populations. We concluded that cholesterol directly affects the lateral mobility *i.e.* fluidity of the lipid bilayer in a temperature dependent manner. Increasing incubation time of a sample of DSPC, above T_M , yielded an increase in SSHH abundance as well as a broadening of the ADH dimer peak corresponding to an increase in cholesterol content in the bilayer. We demonstrated that temperature, cholesterol incorporation, and incubation time play a role in determining the conformer preferences of GA. The utilization of VCFD coupled to IM-MS emphasizes that comparisons can be made to relate changes in various physicochemical interactions with the effects these changes have on peptide/protein structural preferences.

In Chapter V improvements on the VCFD method were described that reduced the sample preparation time by approximated 50 % and allowed for the investigation of GA dimer conformer preferences directly from aqueous suspensions of lipid bilayers. A novel implementation of a mixing tee apparatus coupled to an ESI (MT-ESI) source was described in the methods section of Chapter V. The ability to electrospray GA dimers directly from aqueous suspensions of lipid bilayers was demonstrated for the first time.

Previously, samples required freeze drying to remove any water prior to ESI analysis. While Chapter III and IV demonstrate that the conformer preferences of GA dimers are significantly different upon lipid bilayer association we aimed to interrogate the conformer preferences directly from a lipid bilayer suspended in aqueous solution. It was hypothesized that the drying process involved in VCFD preparation may have some effect on conformer preferences of the GA complex however Chapter V results demonstrate that freeze drying did not significantly affect GA conformer preferences. The conformer preferences of GA from POPC (16:0, 18:1 PC) and DEPC (22:1 PC) lipid bilayers were revealed to be nearly identical when comparing VCFD and MT-ESI results from Chapter IV and V. Modified GA analogues (GA3K and GA3K(ipr)) containing lysine residues substituted for leucine residues at positions 10, 12, and 14 were employed to facilitate studies on i) how conformer preferences change upon the introduction of hydrophilic sites into the sequence, and ii) investigations into interactions between a cationic ion channel complex and negatively charged lipid bilayer containing phosphatidylglycerol (PG) head groups. Chapter V results revealed that the introduction of hydrophilic lysine residues into GA analogues yielded primarily ADH-like conformer preferences when associated with negatively charged headgroup phospholipids.

Future Directions

The utilization of both VCFD and MT-ESI techniques presents a significant opportunity for future investigations. As noted in the discussion on GA conformer preferences in Chapters III and IV, simply changing the identity of the lipids when preparing the lipid bilayers has an effect on the conformer preferences of GA dimers. It

would be fruitful to compile a library wherein the effects of a number of lipids differing by acyl chain length, extent of unsaturation, and headgroup identity are studied. This library could be a useful tool for structural predictions about the conformer that a peptide or protein adopts in a membrane of a given composition. Pharmaceutical companies as well as academic laboratories are deeply interested in the prediction of the behavior of a peptide or protein when interacting with a lipid surface thus libraries as mentioned above could see great utility in the future of these fields. Additionally, only one sterol was investigated in Chapter IV however a great number exist in nature. A study on the effects of sterols such as ergosterol, which is reported to interact differently with lipid headgroups and acyl chains as compared to cholesterol, would yield great insight into how these small molecules affect peptide / protein structure in physiologically relevant environments. The effect of temperature on cholesterol-containing systems was investigated in Chapter IV however this study could be extended during the investigation of different lipids and small molecules again to prepare a library for the prediction of peptide or protein behavior at a given temperature.

The introduction of lysine residues into the GA sequence revealed a distinct change in the conformer preferences of GA dimers towards primarily ADH conformers. While only two analogues were studied in Chapter V a wealth of modified GA analogues exist with varying sidechain basicity. In the future, a range of GA analogues could be investigated to understand the interactions between these sidechains and phospholipid headgroups, backbone carbonyls on GA, and solvent. Understanding these interactions

would further enhance our understanding of the biophysical behavior of GA with its environment and ultimately of ion channels in general.

REFERENCES

1. Hubner, C. A.; Jentsch, T. J. Ion channel diseases. *Hum Mol Genet* **2002**, *11*, 2435-45.
2. Reginster, J. Y.; Burlet, N. Osteoporosis: a still increasing prevalence. *Bone* **2006**, *38*, S4-9.
3. Organization, W. H. Epilepsy Fact Sheet.
<http://www.who.int/mediacentre/factsheets/fs999/en> (accessed September 19, 2016).
4. Worldwide, C. F. 2015 Annual Report. https://www.cfww.org/wp-content/uploads/2016/10/annual_report_2015.pdf (accessed September 19, 2016).
5. Tempel, B. L.; Papazian, D. M.; Schwarz, T. L.; Jan, Y. N.; Jan, L. Y. Sequence of a probable potassium channel component encoded at Shaker locus of *Drosophila*. *Science* **1987**, *237*, 770-5.
6. Cooper, E. C.; Jan, L. Y. Ion channel genes and human neurological disease: recent progress, prospects, and challenges. *Proc Natl Acad Sci U S A* **1999**, *96*, 4759-4766.
7. Jentsch, T. J.; Hubner, C. A.; Fuhrmann, J. C. Ion channels: function unravelled by dysfunction. *Nat Cell Biol* **2004**, *6*, 1039-1047.
8. Fenn, J. B.; Mann, M.; Meng, C. K.; Wong, S. F.; Whitehouse, C. M. Electrospray ionization for mass spectrometry of large biomolecules. *Science* **1989**, *246*, 64-71.
9. Demmers, J. A.; Haverkamp, J.; Heck, A. J.; Koeppe, R. E., 2nd; Killian, J. A. Electrospray ionization mass spectrometry as a tool to analyze hydrogen/deuterium

exchange kinetics of transmembrane peptides in lipid bilayers. *Proc Natl Acad Sci U S A* **2000**, *97*, 3189-3194.

10. Breuker, K.; McLafferty, F. W. Stepwise evolution of protein native structure with electrospray into the gas phase, 10(-12) to 10(2) s. *Proc Natl Acad Sci U S A* **2008**, *105*, 18145-18152.

11. Silveira, J. A.; Servage, K. A.; Gamage, C. M.; Russell, D. H. Cryogenic ion mobility-mass spectrometry captures hydrated ions produced during electrospray ionization. *J Phys Chem A* **2013**, *117*, 953-961.

12. Silveira, J. A.; Fort, K. L.; Kim, D.; Servage, K. A.; Pierson, N. A.; Clemmer, D. E.; Russell, D. H. From solution to the gas phase: stepwise dehydration and kinetic trapping of substance P reveals the origin of peptide conformations. *J Am Chem Soc* **2013**, *135*, 19147-19153.

13. Servage, K. A.; Fort, K. L.; Silveira, J. A.; Shi, L.; Clemmer, D. E.; Russell, D. H. Unfolding of Hydrated Alkyl Diammonium Cations Revealed by Cryogenic Ion Mobility-Mass Spectrometry. *J Am Chem Soc* **2015**, *137*, 8916-8919.

14. Servage, K. A.; Silveira, J. A.; Fort, K. L.; Clemmer, D. E.; Russell, D. H. Water-Mediated Dimerization of Ubiquitin Ions Captured by Cryogenic Ion Mobility-Mass Spectrometry. *J Phys Chem Lett* **2015**, *6*, 4947-4951.

15. Chen, S. H.; Russell, D. H. How Closely Related Are Conformations of Protein Ions Sampled by IM-MS to Native Solution Structures? *J Am Soc Mass Spectr* **2015**, *26*, 1433-1443.

16. Hladky, S. B.; Haydon, D. A. Ion transfer across lipid membranes in the presence of gramicidin A. I. Studies of the unit conductance channel. *Biochim Biophys Acta* **1972**, *274*, 294-312.
17. Veatch, W. R.; Mathies, R.; Eisenberg, M.; Stryer, L. Simultaneous fluorescence and conductance studies of planar bilayer membranes containing a highly active and fluorescent analog of gramicidin A. *J Mol Biol* **1975**, *99*, 75-92.
18. Sychev, S. V.; Barsukov, L. I.; Ivanov, V. T. The double pi pi 5.6 helix of gramicidin A predominates in unsaturated lipid membranes. *Eur Biophys J* **1993**, *22*, 279-288.
19. Prausnitz, M. R.; Mitragotri, S.; Langer, R. Current status and future potential of transdermal drug delivery. *Nat Rev Drug Discov* **2004**, *3*, 115-124.
20. Herce, H. D.; Garcia, A. E. Molecular dynamics simulations suggest a mechanism for translocation of the HIV-1 TAT peptide across lipid membranes. *Proc Natl Acad Sci U S A* **2007**, *104*, 20805-20810.
21. Orsi, M.; Essex, J. W. Permeability of drugs and hormones through a lipid bilayer: insights from dual-resolution molecular dynamics. *Soft Matter* **2010**, *6*, 3797-3808.
22. Xiang, T. X.; Anderson, B. D. Liposomal drug transport: A molecular perspective from molecular dynamics simulations in lipid bilayers. *Adv Drug Deliver Rev* **2006**, *58*, 1357-1378.

23. Reshetnyak, Y. K.; Segala, M.; Andreev, O. A.; Engelman, D. M. A monomeric membrane peptide that lives in three worlds: in solution, attached to, and inserted across lipid bilayers. *Biophys J* **2007**, *93*, 2363-2372.
24. Subczynski, W. K.; Wisniewska, A.; Yin, J. J.; Hyde, J. S.; Kusumi, A. Hydrophobic barriers of lipid bilayer membranes formed by reduction of water penetration by alkyl chain unsaturation and cholesterol. *Biochemistry* **1994**, *33*, 7670-7681.
25. Koeppe, R. E., 2nd; Anderson, O. S. Engineering the gramicidin channel. *Annu Rev Biophys Biomol Struct* **1996**, *25*, 231-258.
26. Killian, J. A.; Prasad, K. U.; Hains, D.; Urry, D. W. The membrane as an environment of minimal interconversion. A circular dichroism study on the solvent dependence of the conformational behavior of gramicidin in diacylphosphatidylcholine model membranes. *Biochemistry* **1988**, *27*, 4848-4855.
27. Coles, J.; Guilhaus, M. Orthogonal Acceleration - a New Direction for Time-of-Flight Mass-Spectrometry - Fast, Sensitive Mass Analysis for Continuous Ion Sources. *Trac-Trend Anal Chem* **1993**, *12*, 203-213.
28. Li, J. W.; Taraszka, J. A.; Counterman, A. E.; Clemmer, D. E. Influence of solvent composition and capillary temperature on the conformations of electrosprayed ions: unfolding of compact ubiquitin conformers from pseudonative and denatured solutions. *Int J Mass Spectrom* **1999**, *185*, 37-47.

29. Snijder, J.; Rose, R. J.; Veesler, D.; Johnson, J. E.; Heck, A. J. R. Studying 18 MDa Virus Assemblies with Native Mass Spectrometry. *Angew Chem Int Edit* **2013**, *52*, 4020-4023.
30. Belov, M. E.; Damoc, E.; Denisov, E.; Compton, P. D.; Horning, S.; Makarov, A. A.; Kelleher, N. L. From Protein Complexes to Subunit Backbone Fragments: A Multi-stage Approach to Native Mass Spectrometry. *Anal Chem* **2013**, *85*, 11163-11173.
31. Mehmood, S.; Allison, T. M.; Robinson, C. V. Mass Spectrometry of Protein Complexes: From Origins to Applications. *Annu Rev Phys Chem* **2015**, *66*, 453-474.
32. Shi, L.; Holliday, A. E.; Glover, M. S.; Ewing, M. A.; Russell, D. H.; Clemmer, D. E. Ion Mobility-Mass Spectrometry Reveals the Energetics of Intermediates that Guide Polyproline Folding. *J Am Soc Mass Spectrom* **2016**, *27*, 22-30.
33. Kebarle, P.; Verkerk, U. H. Electrospray: From Ions in Solution to Ions in the Gas Phase, What We Know Now. *Mass Spectrom Rev* **2009**, *28*, 898-917.
34. Wilm, M.; Mann, M. Analytical properties of the nanoelectrospray ion source. *Anal Chem* **1996**, *68*, 1-8.
35. Gibson, G. T. T.; Mugo, S. M.; Oleschuk, R. D. Nanoelectrospray Emitters: Trends and Perspective. *Mass Spectrom Rev* **2009**, *28*, 918-936.
36. Shvartsburg, A. A.; Hudgins, R. R.; Dugourd, P.; Jarrold, M. F. Structural information from ion mobility measurements: applications to semiconductor clusters. *Chem Soc Rev* **2001**, *30*, 26-35.

37. Fenn, L. S.; Kliman, M.; Mahsut, A.; Zhao, S. R.; McLean, J. A. Characterizing ion mobility-mass spectrometry conformation space for the analysis of complex biological samples. *Anal Bioanal Chem* **2009**, *394*, 235-244.
38. Arora, A.; Abildgaard, F.; Bushweller, J. H.; Tamm, L. K. Structure of outer membrane protein A transmembrane domain by NMR spectroscopy. *Nat Struct Biol* **2001**, *8*, 334-338.
39. Creuzet, F.; Mcdermott, A.; Gebhard, R.; Vanderhoef, K.; Spijkerassink, M. B.; Herzfeld, J.; Lugtenburg, J.; Levitt, M. H.; Griffin, R. G. Determination of Membrane-Protein Structure by Rotational Resonance Nmr - Bacteriorhodopsin. *Science* **1991**, *251*, 783-786.
40. Henderson, R.; Baldwin, J. M.; Ceska, T. A.; Zemlin, F.; Beckmann, E.; Downing, K. H. Model for the structure of bacteriorhodopsin based on high-resolution electron cryo-microscopy. *J Mol Biol* **1990**, *213*, 899-929.
41. Van den Berg, B.; Clemons, W. M., Jr.; Collinson, I.; Modis, Y.; Hartmann, E.; Harrison, S. C.; Rapoport, T. A. X-ray structure of a protein-conducting channel. *Nature* **2004**, *427*, 36-44.
42. Wallace, B. A. Crystallographic studies of a transmembrane ion channel, gramicidin A. *Prog Biophys Mol Biol* **1992**, *57*, 59-69.
43. Doyle, D. A.; Morais Cabral, J.; Pfuetzner, R. A.; Kuo, A.; Gulbis, J. M.; Cohen, S. L.; Chait, B. T.; MacKinnon, R. The structure of the potassium channel: molecular basis of K⁺ conduction and selectivity. *Science* **1998**, *280*, 69-77.

44. Welsh, M. J.; Smith, A. E. Molecular mechanisms of CFTR chloride channel dysfunction in cystic fibrosis. *Cell* **1993**, *73*, 1251-1254.
45. Saravanan, R.; Bhattacharjya, S. Oligomeric structure of a cathelicidin antimicrobial peptide in dodecylphosphocholine micelle determined by NMR spectroscopy. *Biochim Biophys Acta* **2011**, *1808*, 369-381.
46. Dubos, R. J. Studies on a Bactericidal Agent Extracted from a Soil Bacillus : I. Preparation of the Agent. Its Activity in Vitro. *J Exp Med* **1939**, *70*, 1-10.
47. Sarges, R.; Witkop, B. Gramicidin A. V. The Structure of Valine- and Isoleucine-Gramicidin A. *J Am Chem Soc* **1965**, *87*, 2011-2020.
48. Urry, D. W. The gramicidin A transmembrane channel: a proposed pi(L,D) helix. *Proc Natl Acad Sci U S A* **1971**, *68*, 672-676.
49. Kemp, G.; Jacobson, K. A.; Wenner, C. E. Solution and interfacial properties of gramicidin pertinent to its effect on membranes. *Biochim Biophys Acta* **1972**, *255*, 493-501.
50. Weinstein, S.; Wallace, B. A.; Blout, E. R.; Morrow, J. S.; Veatch, W. Conformation of gramicidin A channel in phospholipid vesicles: a ¹³C and ¹⁹F nuclear magnetic resonance study. *Proc Natl Acad Sci U S A* **1979**, *76*, 4230-4234.
51. Townsley, L. E. The three-dimensional structure of gramicidin analogs in micellar environments determined using two-dimensional nuclear magnetic resonance spectroscopic techniques. University of Arkansas.

52. Burkhart, B. M.; Gassman, R. M.; Langs, D. A.; Pangborn, W. A.; Duax, W. L. Heterodimer formation and crystal nucleation of gramicidin D. *Biophys J* **1998**, *75*, 2135-2146.
53. Townsley, L. E.; Tucker, W. A.; Sham, S.; Hinton, J. F. Structures of gramicidins A, B, and C incorporated into sodium dodecyl sulfate micelles. *Biochemistry* **2001**, *40*, 11676-11686.
54. Wallace, B. A. Recent Advances in the High Resolution Structures of Bacterial Channels: Gramicidin A. *J Struct Biol* **1998**, *121*, 123-141.
55. Zhang, H.; Cui, W.; Gross, M. L. Native electrospray ionization and electron-capture dissociation for comparison of protein structure in solution and the gas phase. *Int J Mass Spectrom* **2013**, 354-355.
56. Konijnenberg, A.; Butterer, A.; Sobott, F. Native ion mobility-mass spectrometry and related methods in structural biology. *Biochim Biophys Acta* **2013**, *1834*, 1239-1256.
57. Barrera, N. P.; Robinson, C. V. Advances in the mass spectrometry of membrane proteins: from individual proteins to intact complexes. *Annu Rev Biochem* **2011**, *80*, 247-271.
58. Hoaglund, C. S.; Valentine, S. J.; Sporleder, C. R.; Reilly, J. P.; Clemmer, D. E. Three-dimensional ion mobility/TOFMS analysis of electrosprayed biomolecules. *Anal Chem* **1998**, *70*, 2236-2242.
59. Henderson, S. C.; Valentine, S. J.; Counterman, A. E.; Clemmer, D. E. ESI/ion trap/ion mobility/time-of-flight mass spectrometry for rapid and sensitive analysis of biomolecular mixtures. *Anal Chem* **1999**, *71*, 291-301.

60. Ruotolo, B. T.; Benesch, J. L.; Sandercock, A. M.; Hyung, S. J.; Robinson, C. V. Ion mobility-mass spectrometry analysis of large protein complexes. *Nat Protoc* **2008**, *3*, 1139-1152.
61. Merenbloom, S. I.; Flick, T. G.; Williams, E. R. How hot are your ions in TWAVE ion mobility spectrometry? *J Am Soc Mass Spectrom* **2012**, *23*, 553-562.
62. O'Boyle, F.; Wallace, B. A. The temperature dependence of gramicidin conformational States in octanol. *Protein Pept Lett* **2003**, *10*, 9-17.
63. Chen, Y.; Wallace, B. A. Solvent effects on the conformation and far UV CD spectra of gramicidin. *Biopolymers* **1997**, *42*, 771-781.
64. Chen, L.; Chen, S. H.; Russell, D. H. An experimental study of the solvent-dependent self-assembly/disassembly and conformer preferences of gramicidin A. *Anal Chem* **2013**, *85*, 7826-7833.
65. Laganowsky, A.; Reading, E.; Allison, T. M.; Ulmschneider, M. B.; Degiacomi, M. T.; Baldwin, A. J.; Robinson, C. V. Membrane proteins bind lipids selectively to modulate their structure and function. *Nature* **2014**, *510*, 172-175.
66. Huang, W.; Levitt, D. G. Theoretical calculation of the dielectric constant of a bilayer membrane. *Biophys J* **1977**, *17*, 111-128.
67. Xu, F.; Cross, T. A. Water: foldase activity in catalyzing polypeptide conformational rearrangements. *Proc Natl Acad Sci U S A* **1999**, *96*, 9057-9061.
68. Arseniev, A. S.; Barsukov, I. L.; Bystrov, V. F.; Lomize, A. L.; Ovchinnikov Yu, A. ¹H-NMR study of gramicidin A transmembrane ion channel. Head-to-head right-handed, single-stranded helices. *FEBS Lett* **1985**, *186*, 168-174.

69. Ovchinnikov Y.A., B. V. F., Ivanov V.T. NMR solution conformation of gramicidin A double helix. *FEBS Lett* **1984**, *165*, 51-56.
70. Hu, W.; Cross, T. A. Tryptophan hydrogen bonding and electric dipole moments: functional roles in the gramicidin channel and implications for membrane proteins. *Biochemistry* **1995**, *34*, 14147-14155.
71. Kelkar, D. A.; Chattopadhyay, A. The gramicidin ion channel: a model membrane protein. *Biochim Biophys Acta* **2007**, *1768*, 2011-2025.
72. Lewis, B. A.; Engelman, D. M. Lipid bilayer thickness varies linearly with acyl chain length in fluid phosphatidylcholine vesicles. *J Mol Biol* **1983**, *166*, 211-217.
73. Silvius, J. R.; McElhaney, R. N. Molecular properties of membrane lipids and activity of a membrane adenosine triphosphatase from *Acholeplasma laidlawii* B. *Rev Infect Dis* **1982**, *4 Suppl*, S50-58.
74. Mobashery, N.; Nielsen, C.; Andersen, O. S. The conformational preference of gramicidin channels is a function of lipid bilayer thickness. *FEBS Lett* **1997**, *412*, 15-20.
75. Kucerka, N.; Tristram-Nagle, S.; Nagle, J. F. Structure of fully hydrated fluid phase lipid bilayers with monounsaturated chains. *J Membr Biol* **2005**, *208*, 193-202.
76. Risselada, H. J.; Marrink, S. J. Curvature effects on lipid packing and dynamics in liposomes revealed by coarse grained molecular dynamics simulations. *Phys Chem Chem Phys* **2009**, *11*, 2056-2067.
77. Shinitzky, M.; Barenholz, Y. Fluidity parameters of lipid regions determined by fluorescence polarization. *Biochim Biophys Acta* **1978**, *515*, 367-394.

78. Kim, T.; Lee, K. I.; Morris, P.; Pastor, R. W.; Andersen, O. S.; Im, W. Influence of hydrophobic mismatch on structures and dynamics of gramicidin a and lipid bilayers. *Biophys J* **2012**, *102*, 1551-1560.
79. Lundbaek, J. A.; Collingwood, S. A.; Ingolfsson, H. I.; Kapoor, R.; Andersen, O. S. Lipid bilayer regulation of membrane protein function: gramicidin channels as molecular force probes. *J R Soc Interface* **2010**, *7*, 373-395.
80. Ketchum, R. R.; Lee, K. C.; Huo, S.; Cross, T. A. Macromolecular structural elucidation with solid-state NMR-derived orientational constraints. *J Biomol NMR* **1996**, *8*, 1-14.
81. Gu, H.; Lum, K.; Kim, J. H.; Greathouse, D. V.; Andersen, O. S.; Koeppe, R. E., 2nd The membrane interface dictates different anchor roles for "inner pair" and "outer pair" tryptophan indole rings in gramicidin A channels. *Biochemistry* **2011**, *50*, 4855-4866.
82. Andersen, O. S.; Nielsen, C.; Maer, A. M.; Lundbaek, J. A.; Goulian, M.; Koeppe, R. E., 2nd Ion channels as tools to monitor lipid bilayer-membrane protein interactions: gramicidin channels as molecular force transducers. *Methods Enzymol* **1999**, *294*, 208-224.
83. Martinac, B.; Hamill, O. P. Gramicidin A channels switch between stretch activation and stretch inactivation depending on bilayer thickness. *Proc Natl Acad Sci U S A* **2002**, *99*, 4308-4312.

84. de Groot, B. L.; Tieleman, D. P.; Pohl, P.; Grubmuller, H. Water permeation through gramicidin A: desformylation and the double helix: a molecular dynamics study. *Biophys J* **2002**, *82*, 2934-2942.
85. Adams, J. M. On the release of the formyl group from nascent protein. *J Mol Biol* **1968**, *33*, 571-589.
86. Spector, A. A.; Yorek, M. A. Membrane lipid composition and cellular function. *J Lipid Res* **1985**, *26*, 1015-1035.
87. Lundbaek, J. A. Lipid bilayer-mediated regulation of ion channel function by amphiphilic drugs. *J Gen Physiol* **2008**, *131*, 421-429.
88. Lee, A. G. How lipids and proteins interact in a membrane: a molecular approach. *Mol Biosyst* **2005**, *1*, 203-212.
89. Marsh, D. Protein modulation of lipids, and vice-versa, in membranes. *Biochim Biophys Acta* **2008**, *1778*, 1545-1575.
90. Sackmann, E. Physical basis of trigger processes and membrane structures. In Biological Membranes. In *Biological Membranes*, Chapman, D., Ed. Academic Press: London, UK, **1984**, pp 105-143.
91. Andersen, O. S.; Koeppe, R. E., 2nd Bilayer thickness and membrane protein function: an energetic perspective. *Annu Rev Biophys Biomol Struct* **2007**, *36*, 107-130.
92. Lundbaek, J. A.; Birn, P.; Hansen, A. J.; Sogaard, R.; Nielsen, C.; Girshman, J.; Bruno, M. J.; Tape, S. E.; Egebjerg, J.; Greathouse, D. V.; Mattice, G. L.; Koeppe, R. E., 2nd; Andersen, O. S. Regulation of sodium channel function by bilayer elasticity: the

importance of hydrophobic coupling. Effects of Micelle-forming amphiphiles and cholesterol. *J Gen Physiol* **2004**, *123*, 599-621.

93. Lundbaek, J. A.; Birn, P.; Girshman, J.; Hansen, A. J.; Andersen, O. S. Membrane stiffness and channel function. *Biochemistry* **1996**, *35*, 3825-3830.

94. Wimley, W. C.; Hristova, K. Antimicrobial peptides: successes, challenges and unanswered questions. *J Membr Biol* **2011**, *239*, 27-34.

95. Pascal, S. M.; Cross, T. A. High-resolution structure and dynamic implications for a double-helical gramicidin A conformer. *J Biomol NMR* **1993**, *3*, 495-513.

96. Patrick, J. W.; Gamez, R. C.; Russell, D. H. Elucidation of conformer preferences for a hydrophobic antimicrobial peptide by vesicle capture-freeze-drying: a preparatory method coupled to ion mobility-mass spectrometry. *Anal Chem* **2015**, *87*, 578-583.

97. Wallace, B. A.; Veatch, W. R.; Blout, E. R. Conformation of gramicidin A in phospholipid vesicles: circular dichroism studies of effects of ion binding, chemical modification, and lipid structure. *Biochemistry* **1981**, *20*, 5754-5760.

98. Greathouse, D. V.; Hinton, J. F.; Kim, K. S.; Koeppe, R. E., 2nd Gramicidin A/short-chain phospholipid dispersions: chain length dependence of gramicidin conformation and lipid organization. *Biochemistry* **1994**, *33*, 4291-4299.

99. Galbraith, T. P.; Wallace, B. A. Phospholipid chain length alters the equilibrium between pore and channel forms of gramicidin. *Faraday Discuss* **1998**, 159-164; discussion 225-46.

100. Evans, E., Needham, D. Physical properties of surfactant bilayer membranes: thermal transitions, elasticity, rigidity, cohesion, and colloidal interactions. *J. Phys. Chem.* **1987**, *91*, 4219-4228.
101. Chen, S. H.; Russell, D. H. How Closely Related Are Conformations of Protein Ions Sampled by IM-MS to Native Solution Structures? *J Am Soc Mass Spectrom* **2015**, *26*, 1433-1443.
102. Brown, M. F. Modulation of rhodopsin function by properties of the membrane bilayer. *Chem Phys Lipids* **1994**, *73*, 159-180.
103. Chang, H. M.; Reitstetter, R.; Mason, R. P.; Gruener, R. Attenuation of channel kinetics and conductance by cholesterol: an interpretation using structural stress as a unifying concept. *J Membr Biol* **1995**, *143*, 51-63.
104. Owicki, J. C.; Springgate, M. W.; McConnell, H. M. Theoretical study of protein--lipid interactions in bilayer membranes. *Proc Natl Acad Sci U S A* **1978**, *75*, 1616-1619.
105. Unwin, P. N.; Ennis, P. D. Two configurations of a channel-forming membrane protein. *Nature* **1984**, *307*, 609-613.
106. Unwin, N.; Toyoshima, C.; Kubalek, E. Arrangement of the acetylcholine receptor subunits in the resting and desensitized states, determined by cryoelectron microscopy of crystallized Torpedo postsynaptic membranes. *J Cell Biol* **1988**, *107*, 1123-1138.
107. Patra, M. Lateral pressure profiles in cholesterol-DPPC bilayers. *Eur Biophys J* **2005**, *35*, 79-88.

108. Lundbaek, J. A.; Andersen, O. S. Spring constants for channel-induced lipid bilayer deformations. Estimates using gramicidin channels. *Biophys J* **1999**, *76*, 889-895.
109. Nielsen, C.; Goulian, M.; Andersen, O. S. Energetics of inclusion-induced bilayer deformations. *Biophys J* **1998**, *74*, 1966-1983.
110. Demmers, J. A.; van Duijn, E.; Haverkamp, J.; Greathouse, D. V.; Koeppe, R. E., 2nd; Heck, A. J.; Killian, J. A. Interfacial positioning and stability of transmembrane peptides in lipid bilayers studied by combining hydrogen/deuterium exchange and mass spectrometry. *J Biol Chem* **2001**, *276*, 34501-34508.
111. Durkin, J. T.; Providence, L. L.; Koeppe, R. E., 2nd; Andersen, O. S. Energetics of heterodimer formation among gramicidin analogues with an NH₂-terminal addition or deletion. Consequences of missing a residue at the join in the channel. *J Mol Biol* **1993**, *231*, 1102-1121.
112. Smith, K. A.; Conboy, J. C. A simplified sum-frequency vibrational imaging setup used for imaging lipid bilayer arrays. *Anal Chem* **2012**, *84*, 8122-8126.
113. Hiroaki, S., I. Masashi, H. Takagi, M. Nishimura, T. Miyakawa, K. Kawaguchi, M. Takasu, T. Mizukami, H. Nagao Molecular dynamics study of gramicidin a in lipid bilayer: Structure and lateral pressure profile. *Int. J. Quantum Chem* **2012**, *112*, 3834-3839.
114. Brown, D. A.; London, E. Functions of lipid rafts in biological membranes. *Annu Rev Cell Dev Biol* **1998**, *14*, 111-136.
115. Simons, K.; Ikonen, E. Functional rafts in cell membranes. *Nature* **1997**, *387*, 569-572.

116. Simons, K.; van Meer, G. Lipid sorting in epithelial cells. *Biochemistry* **1988**, *27*, 6197-6202.
117. Mikhailov, V. A.; Liko, I.; Mize, T. H.; Bush, M. F.; Benesch, J. L.; Robinson, C. V. Infrared Laser Activation of Soluble and Membrane Protein Assemblies in the Gas Phase. *Anal Chem* **2016**, *88*, 7060-7067.
118. Gault, J.; Donlan, J. A.; Liko, I.; Hopper, J. T.; Gupta, K.; Housden, N. G.; Struwe, W. B.; Marty, M. T.; Mize, T.; Bechara, C.; Zhu, Y.; Wu, B.; Kleanthous, C.; Belov, M.; Damoc, E.; Makarov, A.; Robinson, C. V. High-resolution mass spectrometry of small molecules bound to membrane proteins. *Nat Methods* **2016**, *13*, 333-336.
119. Samulak, B. M.; Niu, S.; Andrews, P. C.; Ruotolo, B. T. Ion Mobility-Mass Spectrometry Analysis of Cross-Linked Intact Multiprotein Complexes: Enhanced Gas-Phase Stabilities and Altered Dissociation Pathways. *Anal Chem* **2016**, *88*, 5290-5298.
120. Dyachenko, A.; Wang, G. B.; Belov, M.; Makarov, A.; de Jong, R. N.; van den Bremer, E. T. J.; Parren, P. W. H. I.; Heck, A. J. R. Tandem Native Mass-Spectrometry on Antibody-Drug Conjugates and Submillion Da Antibody-Antigen Protein Assemblies on an Orbitrap EMR Equipped with a High-Mass Quadrupole Mass Selector. *Anal Chem* **2015**, *87*, 6095-6102.
121. Cong, X.; Liu, Y.; Liu, W.; Liang, X. W.; Russell, D. H.; Laganowsky, A. Determining Membrane Protein-Lipid Binding Thermodynamics Using Native Mass Spectrometry. *J Am Chem Soc* **2016**, *138*, 4346-4349.

122. Zhang, H.; Harrington, L. B.; Lu, Y.; Prado, M.; Saer, R.; Rempel, D.; Blankenship, R. E.; Gross, M. L. Native Mass Spectrometry Characterizes the Photosynthetic Reaction Center Complex from the Purple Bacterium *Rhodospirillum rubrum*. *J Am Soc Mass Spectrom* **2016**.
123. Marty, M. T.; Zhang, H.; Cui, W. D.; Blankenship, R. E.; Gross, M. L.; Sligar, S. G. Native Mass Spectrometry Characterization of Intact Nanodisc Lipoprotein Complexes. *Anal Chem* **2012**, *84*, 8957-8960.
124. Han, L.; Kitova, E. N.; Li, J.; Nikjah, S.; Lin, H.; Pluvinage, B.; Boraston, A. B.; Klassen, J. S. Protein-Glycolipid Interactions Studied in Vitro Using ESI-MS and Nanodiscs: Insights into the Mechanisms and Energetics of Binding. *Anal Chem* **2015**, *87*, 4888-4896.
125. Leney, A. C.; Fan, X. X.; Kitova, E. N.; Klassen, J. S. Nanodiscs and Electrospray Ionization Mass Spectrometry: A Tool for Screening Glycolipids Against Proteins. *Anal Chem* **2014**, *86*, 5271-5277.
126. Patrick, J. W.; Gamez, R. C.; Russell, D. H. Elucidation of Conformer Preferences for a Hydrophobic Antimicrobial Peptide by Vesicle Capture-Freeze-Drying: A Preparatory Method Coupled to Ion Mobility-Mass Spectrometry. *Anal Chem* **2015**, *87*, 578-583.
127. Patrick, J. W.; Gamez, R. C.; Russell, D. H. The Influence of Lipid Bilayer Physicochemical Properties on Gramicidin A Conformer Preferences. *Biophys J* **2016**, *110*, 1826-1835.

128. Wilson, D. J.; Konermann, L. Mechanistic studies on enzymatic reactions by electrospray ionization MS using a capillary mixer with adjustable reaction chamber volume for time-resolved measurements. *Anal Chem* **2004**, *76*, 2537-2543.
129. Zinck, N.; Stark, A. K.; Wilson, D. J.; Sharon, M. An Improved Rapid Mixing Device for Time-Resolved Electrospray Mass Spectrometry Measurements. *Chemistryopen* **2014**, *3*, 109-114.
130. Ruotolo, B. T.; Benesch, J. L. P.; Sandercock, A. M.; Hyung, S. J.; Robinson, C. V. Ion mobility-mass spectrometry analysis of large protein complexes. *Nat Protoc* **2008**, *3*, 1139-1152.
131. Marty, M. T.; Hoi, K. K.; Gault, J.; Robinson, C. V. Probing the Lipid Annular Belt by Gas-Phase Dissociation of Membrane Proteins in Nanodiscs. *Angew Chem Int Edit* **2016**, *55*, 550-554.
132. Laganowsky, A.; Reading, E.; Hopper, J. T. S.; Robinson, C. V. Mass spectrometry of intact membrane protein complexes. *Nat Protoc* **2013**, *8*, 639-651.
133. Kemp, G.; Wenner, C. E.; Jacobson, K. A. Solution and Interfacial Properties of Gramicidin Pertinent to Its Effect on Membranes. *Biochim Biophys Acta* **1972**, *225*, 493-501.
134. Chen, L. X.; Chen, S. H.; Russell, D. H. An Experimental Study of the Solvent-Dependent Self-Assembly/Disassembly and Conformer Preferences of Gramicidin A. *Anal Chem* **2013**, *85*, 7826-7833.
135. Wallace, B. A. Structure of Gramicidin-A. *Biophys J* **1986**, *49*, 295-306.

136. Smart, O. S.; Goodfellow, J. M.; Wallace, B. A. The Pore Dimensions of Gramicidin-A. *Biophys J* **1993**, *65*, 2455-2460.
137. Galbraith, T. P.; Wallace, B. A. Phospholipid chain length alters the equilibrium between pore and channel forms of gramicidin. *Faraday Discuss* **1998**, *111*, 159-164.
138. Epanand, R. M.; Vogel, H. J. Diversity of antimicrobial peptides and their mechanisms of action. *Bba-Biomembranes* **1999**, *1462*, 11-28.
139. Zerfas, B. L.; Joo, Y.; Gao, J. M. GramicidinA Mutants with Antibiotic Activity against Both Gram-Positive and Gram-Negative Bacteria. *Chemmedchem* **2016**, *11*, 629-636.
140. Wang, F.; Qin, L. H.; Pace, C. J.; Wong, P.; Malonis, R.; Gao, J. M. Solubilized Gramicidin A as Potential Systemic Antibiotics. *Chembiochem* **2012**, *13*, 51-55.
141. Shai, Y. Mechanism of the binding, insertion and destabilization of phospholipid bilayer membranes by alpha-helical antimicrobial and cell non-selective membrane-lytic peptides. *Bba-Biomembranes* **1999**, *1462*, 55-70.
142. Wimley, W. C.; White, S. H. Protein folding in membranes: A peptide designed to spontaneously insert across lipid bilayers. *Biophys J* **1998**, *74*, A16-A16.
143. Patrick, J.W.; Zerfas, B.L.; Gao, J.; Russell, D.H. Rapid capillary mixing experiments for the analysis of hydrophobic membrane complexes directly from aqueous lipid bilayer solutions. *Analyst* **2016** DOI:10.1039/C6AN02290A

APPENDIX

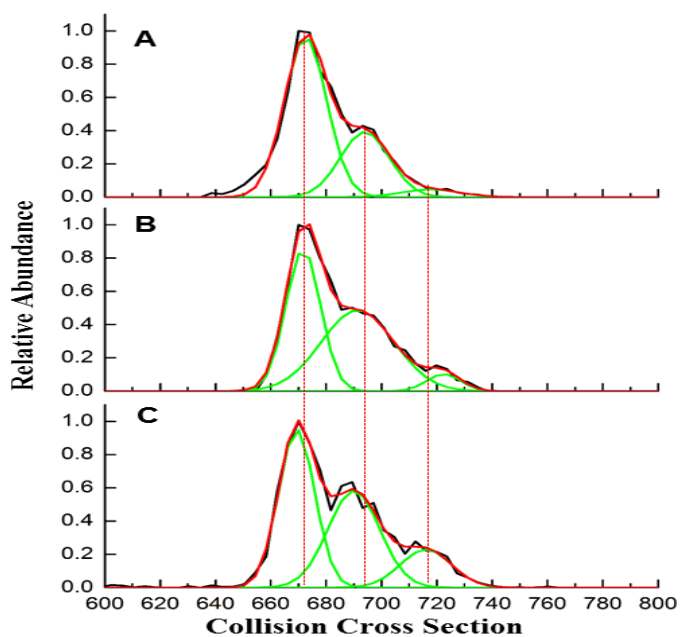


Figure A1. CCS profile for GA $[2\text{GA} + 2\text{Na}]^{2+}$ ions electrosprayed from isobutanol control samples in the presence of A) DLPC (12:0 PC), B) POPC (16:0, 18:1 PC) and C) DEPC (22:1 PC) lipids. CCS profiles displayed are for non-aqueous samples prepared using the VCFD methodology. Comparison to Figure 9, containing aqueous VCFD-prepared GA samples in PC lipids, demonstrates that dramatically different conformer preferences are observed. This data illustrates the utility of using VCFD to yield a different number and/or abundance of conformers not visible by simple ESI analysis.

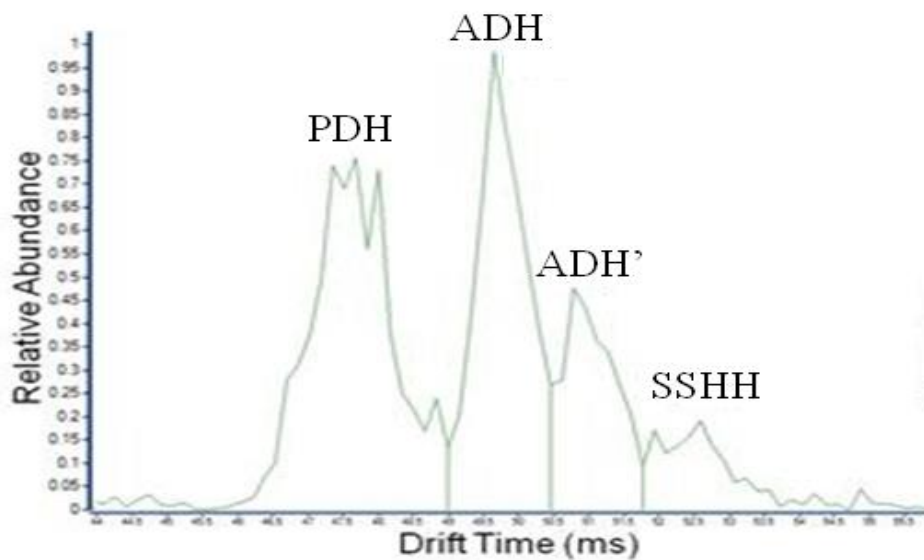


Figure A2. High resolution CCS profile for $[2GA + 2Na]^{2+}$ ions obtained on the Agilent 6560 IM-MS instrument; $R \sim 70$. CCS profiles for ADH are two component and the relative abundances of the two peaks are dependent on the solution environment from which the ions are generated. Note also that at $R \sim 70$ the peak for PDH also shows evidence of a leading edge component for a second peak.

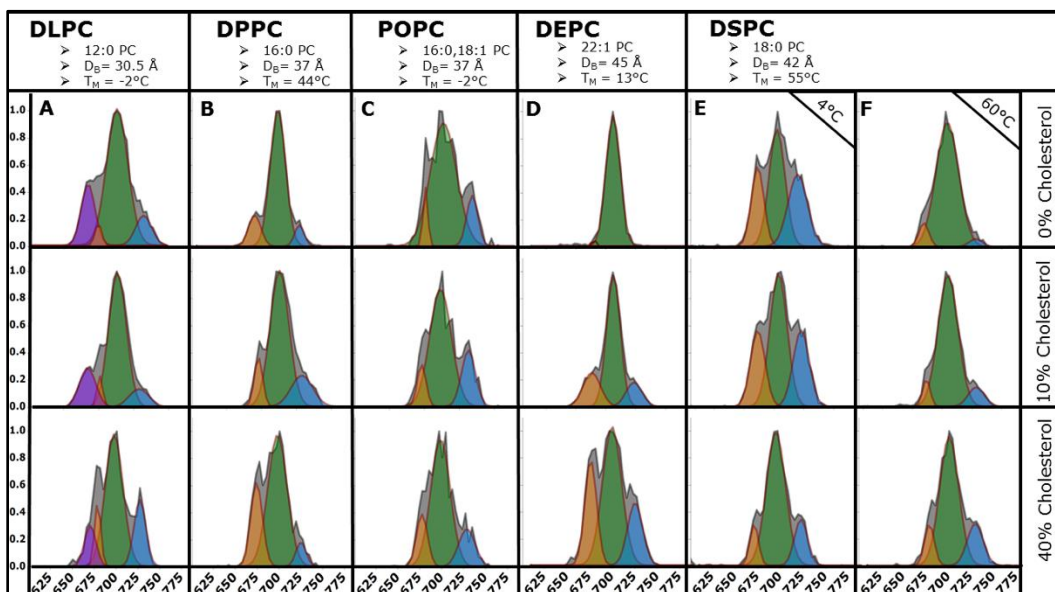


Figure A3. CCS profiles for $[2\text{GA} + 2\text{Na}]^{2+}$ ions electrospayed from 100 nm DLPC (A), DPPC (B), POPC (C), DEPC (D), and DSPC (E-F) vesicles containing 0-40 mol% cholesterol (vertical, shown at right) plotted as relative abundance vs. CCS (\AA^2). Acyl chain designations, lipid bilayer thickness (D_B), and gel-to-liquid phase transition temperatures (T_M) are provided for each lipid. Peaks fit using $n=3$. Conformers have been labeled according to the following scheme: Purple – Nascent conformer (660 \AA^2), Orange – PDH (675 \AA^2), Green – ADH (700 \AA^2), Blue – SSHH (725 \AA^2).

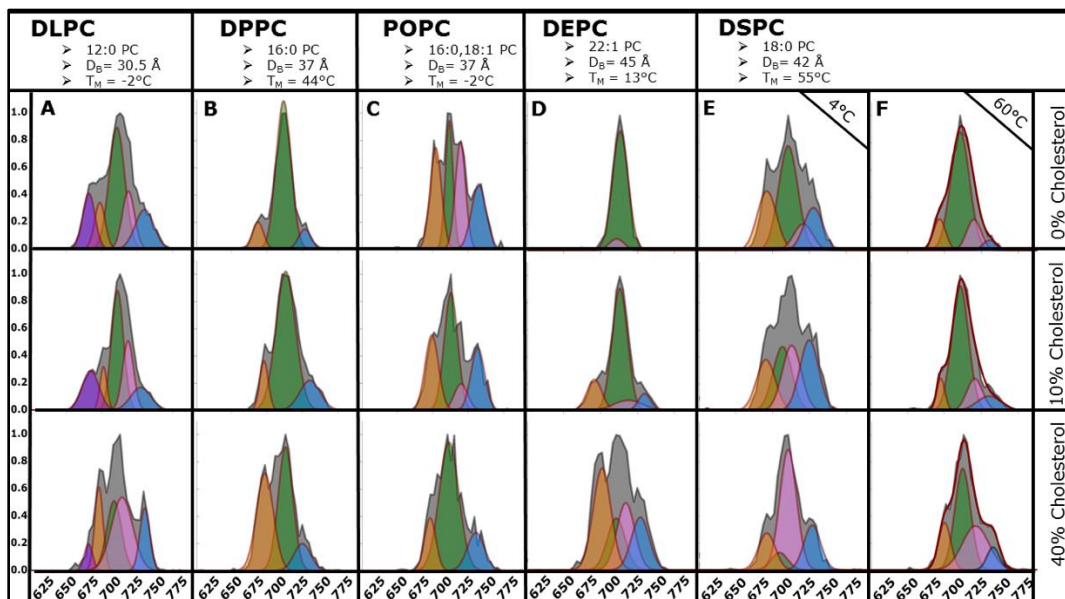


Figure A4. CCS profiles for $[2\text{GA} + 2\text{Na}]^{2+}$ ions electrosprayed from 100 nm DLPC (A), DPPC (B), POPC (C), DEPC (D), and DSPC (E-F) vesicles containing 0-40 mol% cholesterol (vertical, shown at right) plotted as relative abundance vs. CCS (\AA^2). Acyl chain designations, lipid bilayer thickness (DB), and gel-to-liquid phase transition temperatures (T_M) are provided for each lipid. Peaks fit using $n=4$. Conformers have been labeled according to the following scheme: Purple – Nascent conformer (660 \AA^2), Orange – PDH (675 \AA^2), Green, Magenta – ADH (700 \AA^2), Blue – SSHH (725 \AA^2).

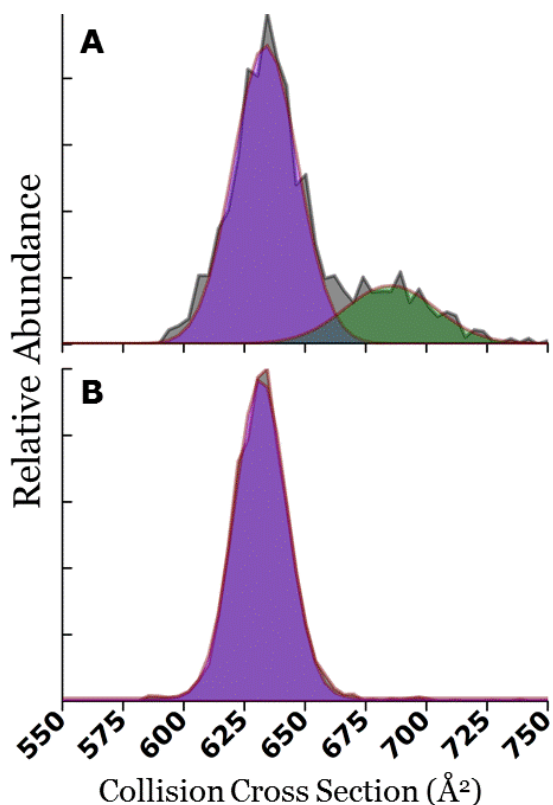


Figure A5. Collision Cross Section profiles for $[2\text{GA3K} + 2\text{Na}]^{2+}$ ions electrosprayed from (A) isobutanol and (B) isobutanol containing 10% water. The predominant conformer adopted by GA3K is shown in purple at *ca.* 635 \AA^2 . Profile B demonstrates that the addition of 10% water to the sample depletes the abundance of the extended GA3K conformer. Conformers have been labeled according to the following scheme: purple, compact conformation (635 \AA^2); green, extended conformations (encompassing PDH, ADH, SSHH) ($\sim 700 \text{ \AA}^2$)